

An ApiAP2 transcription factor influencing virulence gene transcription and sexual development in *Plasmodium falciparum*

Eliana Cubillos

University of Sao Paulo

Isadora Prata

University of Sao Paulo

Wesley Fotoran

University of Sao Paulo

Nicolas Cardenas

University of São Paulo

Diego Alonso

Institute for Biotechnology, UNESP

Paulo Ribolla

Institute for Biotechnology, UNESP

Lisa Ranford-Cartwright

University of Glasgow <https://orcid.org/0000-0003-1992-3940>

Gerhard Wunderlich (✉ gwunder@usp.br)

University of Sao Paulo <https://orcid.org/0000-0003-1724-0337>

Article

Keywords:

Posted Date: August 10th, 2020

DOI: <https://doi.org/10.21203/rs.3.rs-48641/v1>

License:   This work is licensed under a Creative Commons Attribution 4.0 International License.

[Read Full License](#)

1 An ApiAP2 transcription factor influencing virulence gene 2 transcription and sexual development in *Plasmodium falciparum*

3 Eliana FG Cubillos¹, Isadora Oliveira Prata ¹, Wesley Luzetti Fotoran¹, Nicolás Cespedes Cardenas³ ,
4 Diego Alonso², Paulo EM Ribolla², Lisa C. Ranford-Cartwright⁴ and Gerhard Wunderlich^{1,*}

5 1. Department of Parasitology, Institute for Biomedical Sciences, University of São Paulo, Avenida
6 Professor Lineu Prestes, 1374, 05508-000, São Paulo-SP, Brazil.

7 2. Institute for Biotechnology, UNESP, Alameda das Tecomarias, 18607-440, Botucatu-SP, Brazil.

8 3. Department of Preventive Veterinary Medicine and Animal Health, School of Veterinary
9 Medicine and Animal Science. University of São Paulo-SP, Brazil.

10 4. Institute of Biodiversity, Animal Health & Comparative Medicine, College of Medical,
11 Veterinary and Life Science, University of Glasgow, Glasgow G12 8QQ, UK.

12 *to whom correspondence should be sent

13

14 Abstract

15 The human malaria parasite *Plasmodium falciparum* expresses variant PfEMP1 proteins on the
16 infected erythrocyte, which function as ligands for endothelial receptors in capillary vessels, leading to
17 erythrocyte sequestration and severe malaria. The factors that orchestrate the mono-allelic expression
18 of the 50-60 PfEMP1-encoding *var* genes within each parasite genome are still not fully identified.
19 Here, we show that the transcription factor PfAP2-O influences the transcription of *var* genes and other
20 multigenic families. The temporary knockdown of PfAP2-O leads to a complete loss of *var*
21 transcriptional memory and a decrease in cytoadherence. AP2-O-knocked down parasites exhibited
22 also significant reductions in transmission through *Anopheles* mosquitoes. We propose that PfAP2-O
23 is one of the major virulence gene transcriptional regulators and may therefore be exploited as an
24 important target to disrupt severe malaria and block parasite transmission.

25

26 Introduction

27 The human malaria parasite *Plasmodium falciparum* remains a risk to a significant portion of
28 the world's population. Despite the considerable success of control measures, *P. falciparum* still causes
29 around 400000 deaths per year, mainly in the sub-Saharan African countries, where most of the victims
30 are either pregnant women or children under 5 years of age¹. Common approaches for malaria control
31 and elimination are artemisinin-based combination therapies (ACT) to treat blood stages in infected

32 patients, and insecticide-impregnated bed nets to prevent mosquito bites and parasite transmission.
33 Although a significant reduction of malaria cases during the first decades of implementation of the
34 aforementioned measures was achieved, recent studies have demonstrated the emergence of
35 parasites resistant to almost all antimalarial treatments including artemisinin ², and of mosquitoes'
36 resistance to the most commonly-used insecticides – pyrethroids, organochlorines, carbamates, and
37 organophosphates – across different endemic areas ³. Therefore, the study and characterization of
38 new drug targets to interfere in parasite transmission are crucial to achieve long-term malaria
39 eradication ⁴.

40 A major parasite virulence factor is PfEMP1 (*Plasmodium falciparum* erythrocyte membrane
41 protein 1), which consists of proteins expressed on the infected red blood cell surface, encoded by the
42 multicopy *var* gene family ⁵. The *var* genes are expressed in a timely, controlled manner, so that only
43 one or a few *var* genes are transcribed per parasite, which prevents immune clearance by immune
44 responses directed against any single PfEMP1 variant ^{6,7}. Different factors are involved in *var* gene
45 transcription, culminating in a process known as allelic exclusion. Specific sequence elements found in
46 the promoter region recruit *var* 5' upstream regions resulting in co-regulation with other *var* loci ⁸. The
47 *var* intron found in all complete *var* genes appears to bi-directionally transcribe non-coding RNAs
48 which are involved in *var* promoter activity ^{9,10}, although activation or silencing can also be achieved in
49 the absence of this motif ¹¹. GC-rich ncRNAs seem to play a major role in the control of *var* gene
50 expression ^{12,13}, and the exosome related RNase PfrR6 seems to fine-regulate the degradation of
51 these RNAs ¹⁴. Several proteins interact directly or indirectly with *var* 5' upstream regions:
52 Heterochromatin protein 1 (HP-1) is associated with silenced chromatin around the promoter region
53 of *var*, and also with genes involved in the production of sexual/transmission stages of the
54 parasite, known as gametocytes ¹⁵. Accordingly, HP-1 knockdown leads to transcriptional de-
55 repression of *var* genes, disruption of allelic exclusion, and the induction of gametocytogenesis,
56 indicating a link between *var* gene transcription and transmission. Several histone modifications,
57 mostly of lysins in histone 3, can be associated with either activated or silenced *var* loci ¹⁶. A specific
58 DNA helicase, RecQ1, associates with actively-transcribed *var* loci ¹⁷. Based on features such as
59 chromosomal location, protein domain structure and sequence similarities, *var* genes have been
60 classified into three major groups, termed upsA, upsB and upsC ¹⁸ that seem to be subject to specific
61 mechanisms of regulation; for example, the activity of a particular RNase II controls transcription of
62 the upsA subgroup ¹⁹.

63 Members of the ApiAP2 family of plant-like transcription factor proteins have been associated
64 with important processes throughout the entire life-cycle of *Plasmodium*. In the rodent malaria
65 parasite *P. berghei*, parasites lacking the protein encoded by *PbAP2-Sp* (PF14_0633/PF3D7_1466400

66 *P. falciparum* ortholog) were unable to complete the sexual cycle inside the mosquito, as they could
67 not form sporozoites²⁰. *P. berghei* parasites lacking *PbAP2-O* (Pf11_0442/PF3D7_1143100 *P.*
68 *falciparum* ortholog) developed as aberrant ookinetes that were unable to invade the *Anopheles*
69 midgut and form oocysts²¹. In *P. falciparum*, the disruption of *PfAP2-G* (PF3D7_1222600) resulted in a
70 complete loss of gametocyte formation, whereas increased expression led to the increased induction
71 of gametocyte-commitment²². Campbell and colleagues identified domains in three ApiAP2 members
72²³ that showed affinity to specific domains in *var* 5' upstream (5' ups) regions²⁴. One of them
73 (PF3D7_0604100/PfSIP2) was shown to interact with upsB *var* sequences, and it was suggested that
74 this protein has a role in tethering of chromatin²⁵. For the second gene, Martins and colleagues
75 demonstrated an upregulation of clonally-variant genes (*stevor* and *rif*, but not *var*) when the predicted
76 protein, PF3D7_1466400/ApiAP2-exp was truncated²⁶. The role of the third protein,
77 PF3D7_1143100/Pf11_0442, remains unknown in *P. falciparum*. Here, we addressed the function of
78 this protein, named PfAP2-O, in the asexual and sexual cycle of *P. falciparum* and found that it
79 influences transcription of multiple genes including variant gene families and is crucial for parasite
80 transmission to *Anopheles* mosquitoes.

81 Results

82 Decreased quantities of PfAP2-O do not interfere with *P. falciparum* blood-stage growth

83 NF54 parasites were successfully modified by single crossover recombination to contain a
84 destabilizing DD24 domain²⁷ in 3'-position of the *PfAP2-O* open reading frame (Figure 1). Removal of
85 Shield-1 from the cultures led to an ~85% depletion of the corresponding protein in mutant parasites
86 (Figure 1, and Supplementary Table 1). As expected from knockout experiments of the orthologous
87 gene in *P. berghei*, the silencing of this factor did not result in a growth defect after 96 h in the absence
88 of Shield-1 compared to control parasites (Figure 1). This shows that PfAP2-O can be tagged with
89 additional domains and its depletion has no immediate influence on asexual stage parasite survival.
90 Using the GFP-tag in this transgenic strain, we observed a nuclear localization of the protein,
91 exclusively in schizonts (Figure 2).

92 PfAP2-O knockdown leads to diversified transcription number of *var* genes

93 Recombinant AP2-domains of PfAP2-O were predicted to bind to elements found in the 5' ups
94 regions of *var* genes²⁴. To elucidate any influence of PfAP2-O on *var* transcription, we selected clonal
95 parasite populations to dominantly express a single dominant *var* gene (*PF3D7_0412400*) by repeated
96 panning of PfAP2-O-GFP-DD24 trophozoite/schizont-infected RBCs over CHO-CD36 cells, as described
97 previously²⁸ (Figure 3A). After this, we performed the silencing of the PfAP2-O for 96 hours, followed
98 by re-establishment of the protein to observe *var* gene transcripts during knockdown and after
99 reestablishment of PfAP2-O. RNA samples from ring stage-parasites were collected from three

100 differently treated cultures: 1. RNA from panned parasites (initial sample), 2. RNA from parasites with
101 PfAP2-O knockdown by the absence of Shield-1 for two reinvasions, and 3. RNA from parasites two
102 reinvasions after the knockdown and reestablishment of PfAP2-O by addition of Shield-1 (Figure 3).

103 In the absence of Shield-1, several *var* transcripts showed increased relative amounts
104 (*PF3D7_0100300*, *PF3D7_0412900*, *PF3D7_0420700*, *PF3D7_0500100*, *PF3D7_0533100*,
105 *PF3D7_0711700*, *PF3D7_0800100*, *PF3D7_0900100*, *PF3D7_0937600*, *PF3D7_1041300*) while the
106 initially dominant *var* gene transcript *PF3D7_0412400* was less abundant (Figure 3B). When checking
107 for chromosomal location of the differently transcribed *var* genes, we observed transcripts from all *var*
108 subgroups, upsA, upsB and upsC. Furthermore, while most of the differentially transcribed *var* genes
109 showed the 5' ups recognition motifs identified for subdomains of PfAP2-O²⁴, others did not, such as
110 *PF3D7_0937600* and *PF3D7_0800100*. Thus, the depletion of PfAP2-O exerts mostly a de-repressing
111 effect on *var* loci that were not exclusively related to any *var* gene subgroup. Importantly, the
112 continuous Shield-1 treatment itself does not alter *var* transcription or *var* transcription memory, since
113 wildtype NF54 and Shield-1-treated transfectant parasites showed similar *var* transcription patterns
114 after selection on CHO-CD36 cells (Figure 3 C, and data for wild type parasites not shown).

115 **Short-term silencing of PfAP2-O leads to the complete deletion of *var* transcription memory**

116 The *var* transcription memory over multiple reinvasions is believed to be maintained by factors
117 that direct chromatin readers and writers to their respective sites of action. Transcriptional activity of
118 genes is reversibly determined in the specific histone code of methylation and acetylation of histone 3
119 lysins and perhaps others²⁹. If PfAP2-O is acting hierarchically upstream in the events that result in the
120 recruiting of silencing and activating factors, then its knockdown should erase the epigenetic memory
121 of *var* gene transcription. To verify what influence a temporary knockdown of AP2-O had on *var*
122 transcription, we observed the *var* transcript profile when the protein function was re-established by
123 re-adding Shield-1. The pre-silencing predominant active locus *PF3D7_0412400* appeared to be
124 silenced after reestablishment of PfAP2-O. Instead, transcripts from its neighbouring locus
125 *PF3D7_0412700* and from upsA *PF3D7_0400400* were dominantly detected, indicating that the
126 transcriptional *var* memory had been erased. In comparison, cytoadherence-selected parasites that
127 were cultivated on Shield-1 throughout the experiment were still dominantly expressing *var* gene
128 *PF3D7_0412400*, confirming that no spurious global switching event occurred during the growth
129 period (Figure 3C and Supplementary Figure 1).

130 **Depletion of PfAP2-O activates gametocyte-related genes**

131 Several members of the ApiAP2 family have been associated with important processes in the
132 *Plasmodium* life cycle, such as gametocyte commitment (*PfAP2-G/PfAP2-G2*)^{22,30}, liver stage³¹,
133 sporozoite (*PbAP2-SP*)²⁰ and oocyst (*PbAP2-O*)²¹ development, and invasion ligand transcription

134 (*PfAP2-I*)³². Considering its role in the transformation to ookinetes in *P. berghei*, we tested if the
135 knockdown of PfAP2-O regulated any of the gametocyte-related transcripts induced by PfAP2-G as well
136 as the transcript of PfAP2-G itself. Interestingly, the PfAP2-O silencing had a mixed effect on
137 gametocyte-associated transcripts in trophozoite stage parasites. While no difference was discernible
138 in the steady-state transcript quantities of PfAP2-G (*PF3D7_1222600*), several key gene transcripts
139 previously associated with gametocyte development appeared in increased amounts (Figure 4A). The
140 transcript of the early gametocyte-expressed gene *Pfs16* (*Pf3D7_0406200*) appeared increased up to
141 4-fold when compared with the control. When the PfAP2-O protein was re-established, we observed
142 that most of the transcripts returned to previous expression levels, with the exception of *Pfs16*, which
143 remained at high levels. To investigate if the *Pfs16* transcript was indeed being translated, its
144 corresponding protein was detected with a specific antibody. While during PfAP2-O-GFP knockdown
145 *Pfs16* was readily detected, re-establishment of PfAP2-O-GFP (Figure 4B) resulted in the disappearance
146 of the protein. Thus, PfAP2-O may also be involved in the regulation of translation of at least *Pfs16*.

147 **Massive parallel transcript analysis identifies targets of PfAP2-O**

148 Other transcripts may be influenced during temporary silencing of PfAP2-O. To address this,
149 we performed an RNA-seq analysis and compared the genome-wide transcriptional profile under three
150 different conditions, exactly as was done with the *var* analysis. We detected 512 upregulated
151 transcripts when the PfAP2-O protein was depleted by Shield-1 removal. Among them, several
152 members of the multigenic families *rifin*, *stevor* and *surfin* as well as alleles of the PHIST family were
153 identified (Figure 5). We also observed 101 downregulated genes, including the early gametocyte
154 marker *PF3D7_0936600.1/PfGEXP5*, another AP2 domain containing protein (*PF3D7_0934400*), a
155 bromodomain containing protein (*PF3D7_1212900*) and the translocon component *PTEX88*
156 (*PF3D7_1105600*) (Supplementary Table 2).

157 Furthermore, we observed a reversal of this effect in PfAP2-O-reestablished parasites since
158 most of the initially upregulated *rifin*, *stevor*, *surfin*, and *phist* transcripts returned to pre-silencing
159 levels. Of the 512 transcripts that were significantly more abundant during knockdown of PfAP2-O,
160 only 16 remained significantly more abundant after PfAP2-O reestablishment, while only four
161 transcripts remained less abundant than the control sample. The *surf* transcripts
162 *PF3D7_1301800.1/Surfin 13.1* and *PF3D7_0402200.1/Surfin 4.1* were still present in higher quantities
163 when AP2-O was re-established. Also, a *rifin* member (*PF3D7_0401600*) that was not altered during
164 Shield-1 removal, was upregulated in PfAP2-O-reestablished parasites (Supplementary figure 2, and
165 Supplementary table 2), indicating transcriptional switching. Therefore, the transcriptional profile of
166 other multigenic families also changed during and after temporary PfAP2-O silencing, as observed by
167 qPCR for *var* genes. Using tools available on plasmodb.org we searched for the predicted PfAP2-O
168 binding motifs 1000 nucleotides upstream of the coding regions of all differentially regulated genes in

169 the control samples versus the knocked down samples and identified 49 with these target motifs,
170 including members of *var*, *surfin* and *rif* (Supplementary Table 3) and PfAP2-O itself. Of note, the PfAP2-
171 O transcript is slightly but significantly more abundant in parasites under PfAP2-O protein knockdown
172 (Supplementary Table 2).

173 In global terms, most of the transcripts that were more abundant in PfAP2-O knocked down
174 parasites compared to control samples, were also significantly less abundant upon recovery and
175 reestablishment of PfAP2-O (n=372). Similarly, of the 101 transcripts that were less abundant upon
176 knockdown of PfAP2-O, 55 were significantly more abundant in PfAP2-O re-established parasites
177 (Supplementary Table 2), and only four remained less abundant after recovery. This shows a reversible
178 modification of multiple transcripts dependent upon the presence or partial absence of PfAP2-O, but
179 also a delayed effect in the case of transcripts that did not return to initial quantities.

180 **Absence of PfAP2-O modifies the cytoadherence phenotype**

181 A landmark of different types of severe malaria is the adherence of infected red blood cells
182 (IRBC) to determined receptors. Considering the observation that the PF3D7_0412400 *var* transcript
183 was much less abundant in a transient knockdown of PfAP2-O, we tested if the parasites also lost the
184 CHO-CD36 adherent phenotype. For this, a static cytoadherence procedure was conducted during and
185 after knockdown. Both CHO-CD36 cells and parasites were counted (Figure 6). We observed that during
186 and after silencing of PfAP2-O the number of parasites adhering to CHO-CD36 cells was significantly
187 lower than the initially CHO-CD36 selected parasites and also the control parasite line, indicating that
188 this factor may influence *P. falciparum* antigenic variation mediated by PfEMP1 proteins.

189 **PfAP2-O interacts with histone modifiers**

190 PfAP2-O probably interacts with other factors to exert its biological role. To identify proteins
191 that physically interact with PfAP2-O, a total protein extract was prepared and the protein complex
192 was immunoprecipitated via the HA tag and purified. Three protein bands at molecular weights of 70,
193 30 and 15 kDa (which did not appear in NF54 wildtype extracts immunoprecipitated in parallel) were
194 detected and analyzed by mass spectrometry (Supplementary Figure 3). In all of these extracts,
195 fragments of a 167 kDa protein appeared and this protein (PF3D7_0216700/PFB0765w) was predicted
196 to be related to autophagy. Fragments of an essential 402 kDa protein with unknown function
197 (PF3D7_0317300/PFC0650w) was detected in the 70 kDa and the 15 kDa fractions. We also observed
198 that PfAP2-O associated with several histone modifiers such as histone-lysine N-methyltransferases
199 SET1 (encoded by *PF3D7_0629700*) and SET2 (encoded by *PF3D7_1322100*, PfSET2/PfSET-VS) and
200 another member of the ApiAP2 family (*PF3D7_0420300*, Supplementary table 4). Intriguingly, no
201 peptides from histones were identified in this assay, indicating that PfAP2-O may not directly interact
202 with these.

203 **PfAP2-O is essential for *P. falciparum* sexual development**

204 The *P. berghei* AP2-O protein (PbApiAP2-O) was associated with mosquito transmission, since
205 knockout parasites for this protein could not form functional ookinetes capable of invading the
206 *Anopheles* midgut and thus completing the sporogonic cycle²¹. We then asked whether the PfAP2-O
207 protein would have the same effect in *P. falciparum*. For this, *Anopheles coluzzii* mosquitoes were fed
208 with the PfAP2-O-GFP-DD24 strain without Shield-1 (AP2-O *knockdown*, KD) and the prevalence of
209 infected mosquitoes and oocyst number was measured and compared with the NF54 WT strain. In all
210 experimental feedings, the infection prevalence was lower than 10% for the KD strain and higher than
211 40% for the WT (Figure 7 A). Using a generalized linear mixed model (GLMM) (Supplementary file 1) to
212 predict the effects of PfAP2-O knockdown on parasite transmission, we observed a significantly lower
213 oocyst prevalence in mosquitoes infected with the PfAP2-O knockdown line compared to the NF54
214 wild type (P-value: 2.6×10^{-6}), controlling for gametocyte numbers in the infectious blood meal which
215 were positively correlated with infection (P=0.0158). The odds ratio values indicated that mosquitoes
216 fed blood meals containing knockdown parasites had a significantly lower probability of infection than
217 those fed with the WT parasites (OR: 0.09). We also observed that a higher number of gametocytes in
218 the infectious blood meal correlated with increased chances of infection (OR: 1.56).

219 When the intensity of the infection (oocyst numbers) in mosquitoes was analysed, we
220 observed that in all experiments, the number of oocysts in mosquitoes fed with KD parasites was
221 significantly lower compared to those fed with the NF54 WT parasites (Figure 7 C). In a GLMM analysis,
222 infection intensity (Supplementary file 1) was significantly influenced by the parasite clone used
223 (P= 5.61×10^{-14}), but not by the gametocyte number in the blood meal (P: 0.0541) (Figure 7 D).

224 These data show that the knockdown of PfApiAP2-O significantly decreased both the
225 prevalence and the intensity of infection in mosquitoes, and predicts a positive relation between the
226 expression of the protein and the transmission of *P. falciparum* from human to *Anopheles* mosquitoes.

227 **Discussion**

228 Transcriptional regulation in *Plasmodium* is typically related to chromatin modification and in
229 this regard, histone methyltransferases, demethylases, histone acetyltransferase and deacetylases
230 have a central role^{33,34}. In the case of *var* genes, however, the hierarchy of events that finally leads to
231 the selective activation of one promoter and the inactivation of the previously active one (switching)
232 is unclear, as is the participation of other factors besides chromatin modifiers. During asexual growth,
233 the histone modification H3K4me2 is known to mark promoters temporarily inactive in trophozoites
234 and schizonts for transcription after the next reinvasion²⁹. Probably just before transcription, a DNA
235 helicase – RecQ1 – is recruited to the to-be-activated *var* site¹⁷, perhaps mediated by an interaction
236 of factors loaded with antisense ncRNAs stemming from the promoter activity localized in the *var*

237 intron^{9,10,35} or with GC-rich ncRNAs¹³. HP1 is found at transcriptionally silenced sites in the genome
238 and is believed to recruit deacetylases and methyl-histone transferases¹⁵, which then modify *var*-
239 associated chromatin (H3K9me3), by the action of at least SIR2A/B^{33,36}. For a number of *upsA var* loci,
240 a special RNase, PfrRNase II, plays a role in silencing *upsA* derived transcripts¹⁹. The concentration of
241 ncRNA RUF6 from different loci seems to play a general role in silencing heterochromatic genes such
242 as *var*, *rif* and others, given that the knockdown of the RNase PfrRp6 leads to generalized de-
243 repression of heterochromatin¹⁴. We hypothesized that by using temporary knockdown of factors
244 putatively participating in these events, the hierarchy of factors playing a role in maintenance or
245 modification of epigenetic signatures of *var* transcription might be elucidated.

246 Here, we show that PfAP2-O, in contrast to its orthologue PbAP2-O, is expressed in schizont
247 stage parasites, already indicating additional roles besides the control of expression of female
248 gametocyte- and ookinete-related genes²¹. Yuda and colleagues showed a translational repression of
249 the PbAP2-O transcript by PbDOZI, which is not the case for the *P. falciparum* orthologue, since it is
250 clearly expressed in schizonts. Intriguingly, but possibly due to its low abundance, PfAP2-O was also
251 not detected in the nuclear proteome of either ring, trophozoite or schizont stages³⁷. Similarly to
252 PbAP2-O, PfAP2-O was also not essential for asexual proliferation, and long-term growth in the
253 absence of Shield-1 revealed no change in parasite development or growth rate during the asexual
254 intraerythrocytic cycle.

255 The knockdown of PfAP2-O led to a swift and complete change of *var* transcription patterns,
256 indicating that PfAP2-O is decisively involved in maintaining the transcriptional memory and acts as an
257 important factor in *var* switching. Based on the results of previous work^{29,38,39}, we hypothesize that
258 histone lysine 9 modifications (trimethylation or acetylation) are different at *var* loci before and after
259 knockdown of PfAP2-O. In consequence, PfAP2-O seems to guide mostly inactivating, chromatin-
260 modifying factors to loci, since in the absence of PfAP2-O, a number of *var* and *rif* loci - but not all - are
261 actively transcribed. It is intriguing that the transcript analysis revealed that the same *var* loci were
262 activated in three biological replicates. Thus, it appears that parasites with activated *var* locus
263 *Pf3D7_0412400* preferentially switch to the same *var* loci identified above when PfAP2-O is
264 temporarily unavailable or available in decreased quantities. Interestingly, when the predicted binding
265 motifs for PfAP2-O were explored in the deregulated genes, only 49 possessed the binding motif
266 (Supplementary table 3.1). A similar observation was described for PfAP2-exp, another member of the
267 ApiAP2 family that was also associated with the control of several gene families²⁶. These data suggest
268 that the binding predictions of motifs for partial AP2 domains may be different from the binding
269 activities of the respective holoproteins.

270 The change of *var* transcription was also reflected in the change of cytoadherence patterns in
271 parasites subjected to PfAP2-O protein depletion. Here, IRBC under PfAP2-O knockdown adhered
272 significantly less to CHO-CD36 cells, probably due to the virtual disappearance of the PfEMP1 that most
273 effectively binds CD36, encoded by *Pf3D7_0412400*. Taking into account that IRBC binding to CHO-
274 CD36 occurred in fact via CD36 and not via other unrelated receptors found on CHO cells ⁴⁰, then
275 interaction with the surface of CHO-CD36 cells of the PfEMP1 ectodomain present in *Pf3D7_0412400*
276 is apparently stronger than that of the *Pf3D7_0412700* ectodomain. Both PfEMP1 ectodomains were
277 predicted to be competent for CD36 binding, while the second most transcribed *var Pf3D7_0400400*
278 encodes a CIDR α 1.1 domain, which is binding to CD36 ⁴¹. The *var Pf3D7_0400400*, upregulated after
279 knockdown and recovery of PfAP2-O, is the so-called *var_{severe}* ⁴² of the upsA *var* group of which
280 expression is upregulated in severe malaria cases ⁴³ and in the onset of infection in non-immune
281 individuals ⁴⁴. In endemic areas, the disruption of cytoadherence remains a challenge in the treatment
282 of patients with severe malaria ⁴⁵. The fact that the plant like ApiAP2 proteins are not encoded in the
283 human host may point PfAP2-O to a novel target of intervention to block the adhesion of infected red
284 blood cells, possibly alleviating life-threatening cytoadherence patterns.

285 Histone protein 1 (HP-1) has previously been shown to control transcription of gametocyte-
286 associated genes by de-repression of *PfAP2-G*, but also that of variant genes such as *var*, *rif* and *Pfmc-*
287 *2TM* ¹⁵. Here, we demonstrated a similar effect with the PfAP2-O factor, which appears to be
288 independent of HP1, since no association between PfAP2-O and HP1 was observed by transcriptomic
289 or proteomic analysis. Based on the upregulation of *var*, *rif*, *stevor*, *PHIST* and *surfin* genes, as well as
290 some gametocyte-associated genes when the PfAP2-O is depleted, we hypothesize that PfAP2-O exerts
291 a repressing effect on several multigenic families and gametocyte markers. These observations
292 underscore the role of this factor in transcriptional memory, not exclusively for *var* genes, but also its
293 involvement in the control of other gene families. PfAP2-O could promote the recruitment of HP-1 to
294 specific sites, which then leads to gene silencing; in the absence of PfAP2-O, the HP-1-guiding effect
295 would then be impaired at least for a number of loci. The role of PfAP2-O in variant gene control is
296 further supported by the observation that different histone modifiers such as PfSET1 and also PfSET2
297 co-precipitated with PfAP2-O, since these have already been linked to *var* transcription ⁴⁶. Importantly,
298 the transcripts of other DNA and RNA binding factors (Supplementary table 2) were differentially
299 present in parasites with knocked-down PfAP2-O and these may play roles in the effects observed
300 here.

301 Regarding sexual commitment, we detected the increased presence of several early
302 gametocyte-related transcripts in PfAP2-O knocked-down parasites. Transcription of the early
303 gametocyte gene *Pfs16 (Pf3D7_0406200)* was strongly increased upon PfAP2-O knockdown, but did

304 not return to pre-knockdown levels after re-exposure of the parasites to Shield1. This may indicate the
305 passing of some as-yet undiscovered checkpoint that leads to persisting *Pfs16* transcription. However,
306 despite the persistence of *Pfs16* transcript, Pfs16 protein was no longer detected after re-
307 establishment of PfAP2-O, suggesting additional post-transcriptional control to prevent translation of
308 this protein when PfAP2-O is present. Of note, post-transcriptional control of Pfs16 has been previously
309 described⁴⁷, but translational repression of Pfs16 seems not to be influenced by the RNA helicase DOZI
310⁴⁸. This suggests that other RNA helicases or factors are involved in the regulation of Pfs16 translation,
311 and that these are directly or indirectly influenced by PfAP2-O.

312 Commitment to gametocyte development is known to be controlled by another member of
313 the ApiAP2 family, PfAP2-G/PF3D7_1222600²²: Increases in PfAP2-G leads to increased transcription
314 of gametocyte-related genes and conversion to gametocytes. The increased expression of PfAP2-G had
315 no significant influence on the transcription of *PfAP2-O*⁴⁹, conversely, we observed that knockdown
316 of PfAP2-O had no enhancing effect on the presence of the *PfAP2-G* transcript. Of note, the earliest
317 gametocyte marker detected so far, gametocyte development protein 1 (GDV-1,⁵⁰), was slightly but
318 significantly downregulated in PfAP2-O knockdowns, reinforcing that PfAP2-O plays no decisive role in
319 gametocyte induction.

320 We also investigated the role of PfAP2-O in parasite transmission through mosquito infection.
321 There was no difference in the number of mature gametocytes obtained under standard culturing
322 conditions for the WT and KD clones (supplementary Figure 4). Furthermore, the gametocytes
323 produced by the PfApiAP2-O knocked down line did not present any difference in shape or size
324 compared to the NF54, which indicates that this protein does not play an important role in gametocyte
325 commitment, however is still uncertain whether these gametocytes have a biological defect that blocks
326 the fertilization and mosquito midgut invasion. In these experiments, we did not study fertilization and
327 ookinete formation to assess this question due to the difficulties to induce them *in vitro* in *P.*
328 *falciparum*. Our results showed that mosquitoes fed with the PfApiAP2-O strain under knockdown had
329 a lower level of infection than those fed with the NF54 WT control, similar to the results shown for the
330 PfAP2-O ortholog in *P. berghei*²¹. We showed that protein depletion of PfApiAP2-O led to a significant
331 decrease in the prevalence of infected mosquitoes as well as a reduction of oocyst numbers. Thus,
332 PfAP2-O appears to be essential for mosquito invasive stages, as was shown for its ortholog in *P.*
333 *berghei*²¹. These observations suggest a conservative role of this protein in human-mosquito
334 transmission among *Plasmodium* species. Finally, the ApiAP2-O knockdown did not result in complete
335 blockade of mosquito infection: a minority of mosquitoes still was infected, with very low oocyst
336 numbers. This could be explained by the fact that the knockdown is not complete and small amounts
337 of protein are detected during Shield withdrawal.

338 Interactions between ApiAP2 proteins in *P. berghei* are involved in crucial processes during
339 the parasite life cycle, including gametocyte development, and oocyst and sporozoite formation⁵¹. In
340 our proteomic co-immunoprecipitation analysis another ApiAP2 member,
341 *PF3D7_0420300/PFD0985W*, with no defined function, was also detected. Campbell and colleagues
342 identified a significant number of target genes predicted for this protein, mainly associated with DNA
343 replication and gene expression²⁴. When binding site evidence for this factor were analyzed in
344 differentially regulated genes in the PfAP2-O knockdown background, we observed 106 targets (more
345 than twice the number that was observed for PfAP2-O) with at least one binding motif (Supplementary
346 Table 3), most of them associated to the cellular processes mentioned by Campbell and colleagues.
347 This evidence leads us to hypothesize that these members may be part of a protein interaction network
348 responsible for important steps in *P. falciparum* life cycle, similar to that described in the murine
349 parasite model.

350 In conclusion, we showed that PfAP2-O controls transcript levels of clonally variant gene
351 families, antigenic variation and transcriptional memory in *P. falciparum* asexual cycle. We also
352 demonstrated a significant decrease in *P. falciparum* transmission to *Anopheles* mosquitos when this
353 protein is absent. PfAP2-O probably interacts with other transcription factors and histone modifiers in
354 a dynamic protein complex involved in several key processes in *P. falciparum* biology. These results
355 highlight PfAP2-O as an attractive drug target to alleviate virulence factor-induced pathogenesis, with
356 additional impacts through blocking the transmission of the parasite from infected human to the
357 invertebrate host.

358

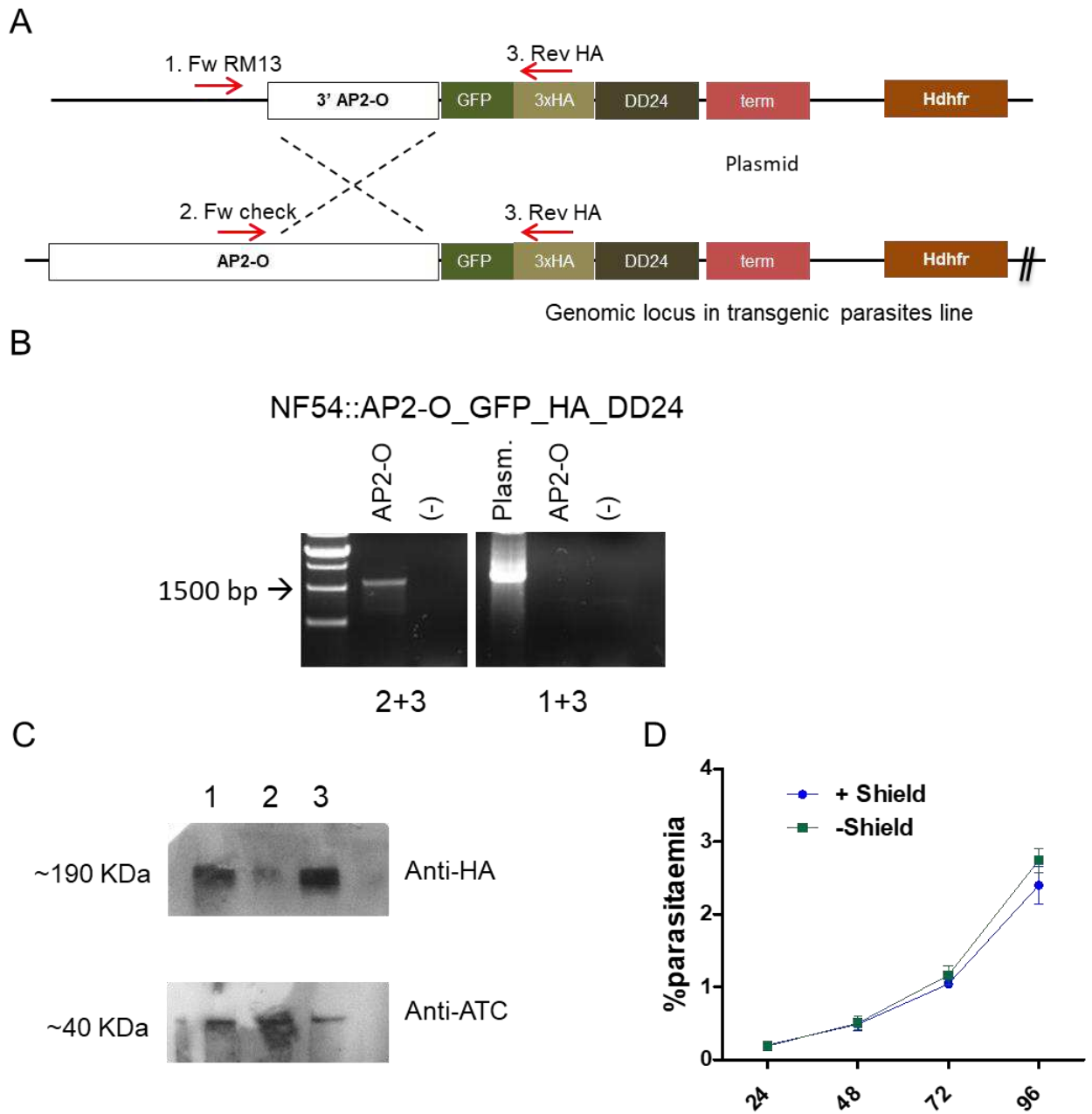


Figure 1. PfAP2-O modification and subsequent knockdown leads to no discernible growth phenotype. **A:** The plasmid structure and its integration of tags by homologous recombination after transfection and cloning is shown. **B:** PCR analysis to confirm the correct integration of the plasmid. The oligonucleotides indicated in **A** resulted in the presence of the expected amplicons. Amplicons using oligo pair 2+3 indicate successful integration, while products using pair 1+3 indicate the presence of episomal forms. **C:** Western blot using anti-HA antibody to detect PfAP2-O-GFP expression in parasites submitted to temporary knockdown by the absence of Shield-1. Lane 1: Parasites grown in the presence of Shield-1, Lane 2: Parasites grown for two reinvasions without Shield-1, lane 3: Parasites after re-establishment of PfAP2-O-GFP by re-addition of Shield-1 for two reinvasion cycles. As a loading control, a polyclonal antiATC (plasmodial aspartate carbamoyltransferase) was used. **D:** Growth curves from NF54::PfAP2-O_GFP_HA_DD24 with and without 0.5 μ M Shield-1 (data from triplicates)

Figure 2

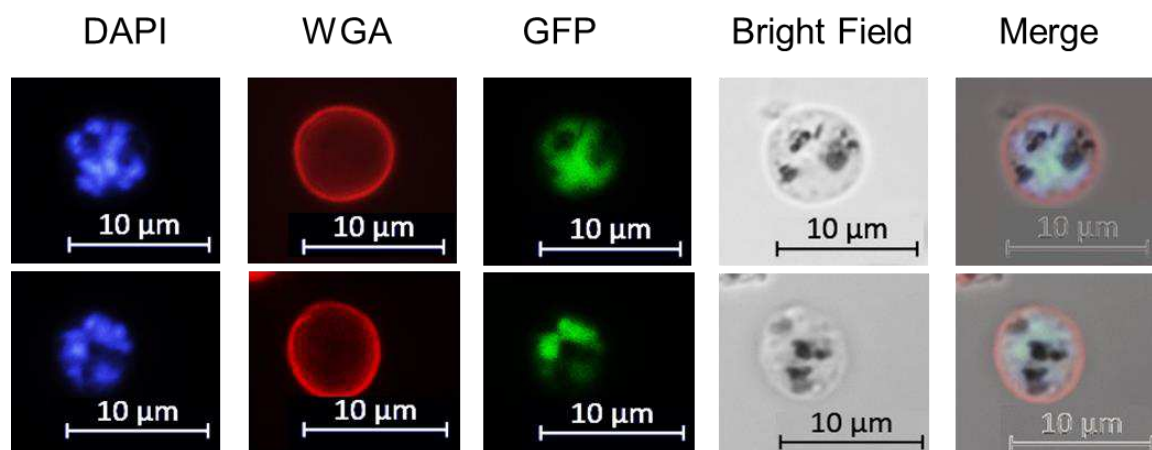
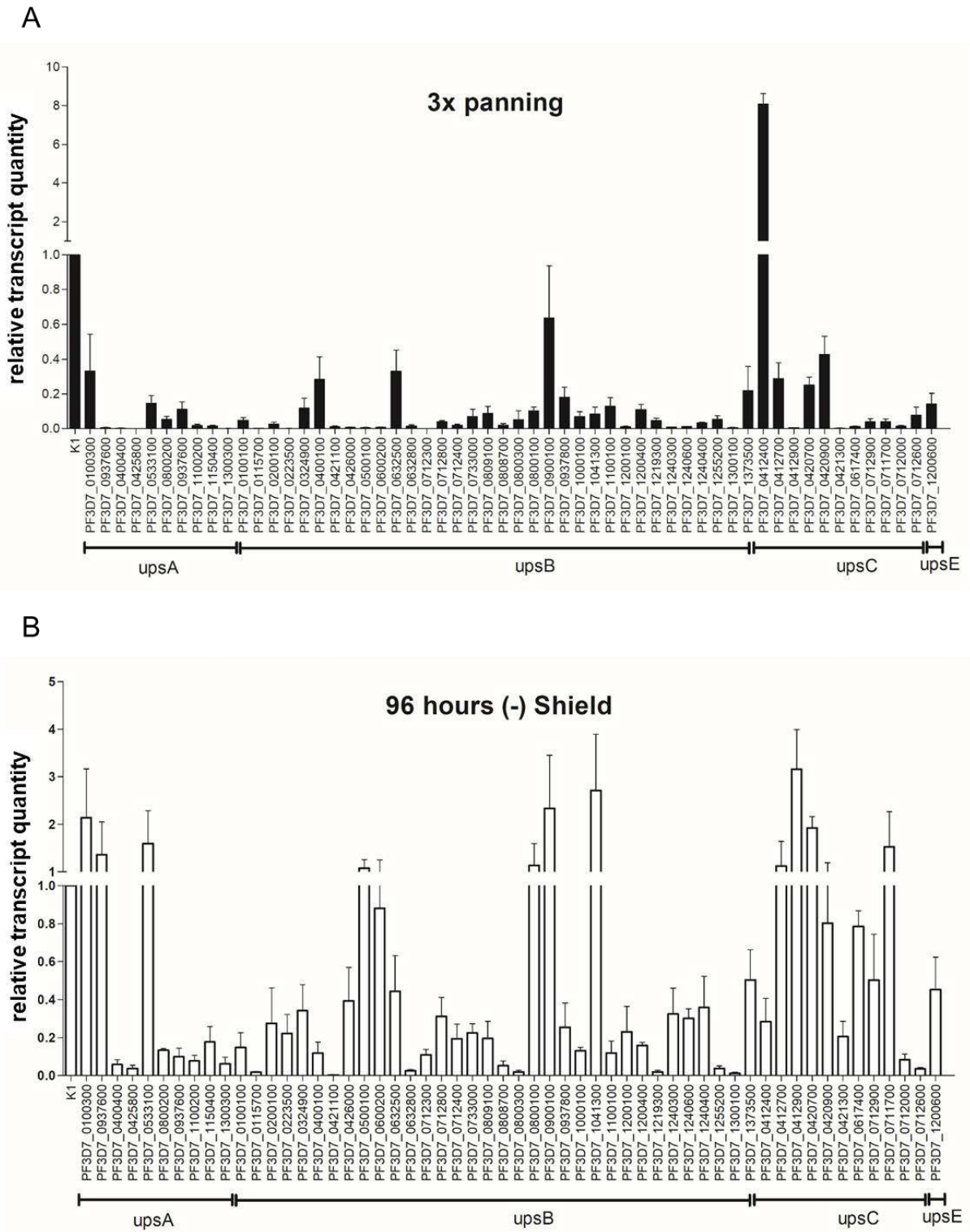


Figure 2: PfAP2-O-GFP-HA-DD24 is expressed in schizont stage parasites. A: Fluorescence microscopy of late schizont parasites shows that GFP-tagged PfAP2-O colocalizes with the DAPI (nuclear stain) signal. WGA marks the surface of red blood cells.

Figure 3



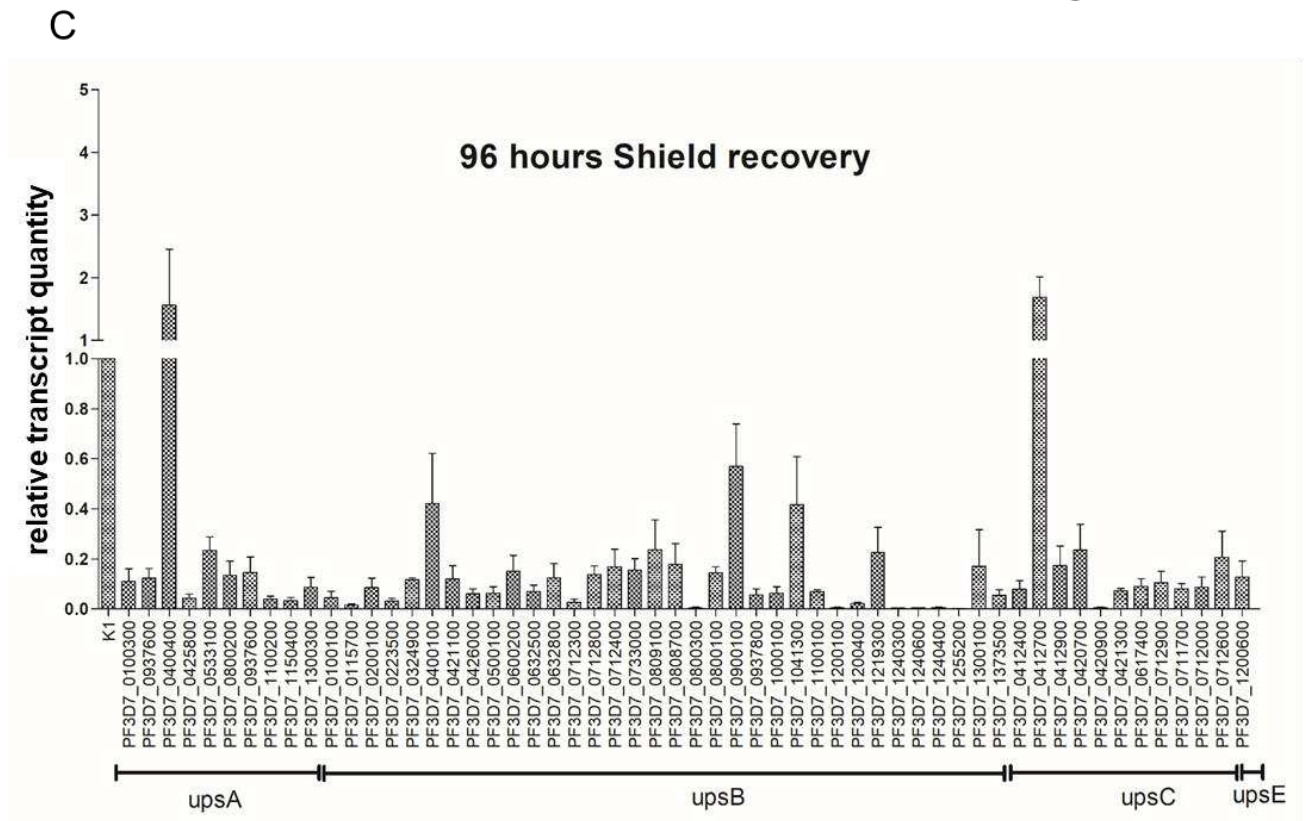


Figure 3: *var* gene transcription analysis during a transient *knockdown* in PfAP2-O-GFP-HA-DD24 parasites. A: RNAs extracted from NF54::PfAP2-O-GFP-DD24 parasites grown in the presence of Shield-1 and panned three times over CHO-CD36 cells were analyzed by RT-qPCR using t-seryl ligase (“K1”) as an internal control transcript, as described in Methods. **B:** *var* transcript profile after 96 hours incubation of parasites without Shield-1. **C:** *var* transcript profile in parasites after re-establishment of PfAP2-O for two reinvasions (96 h). The data represent results from three independent experiments and error bars indicate the standard deviation between these.

Figure 4

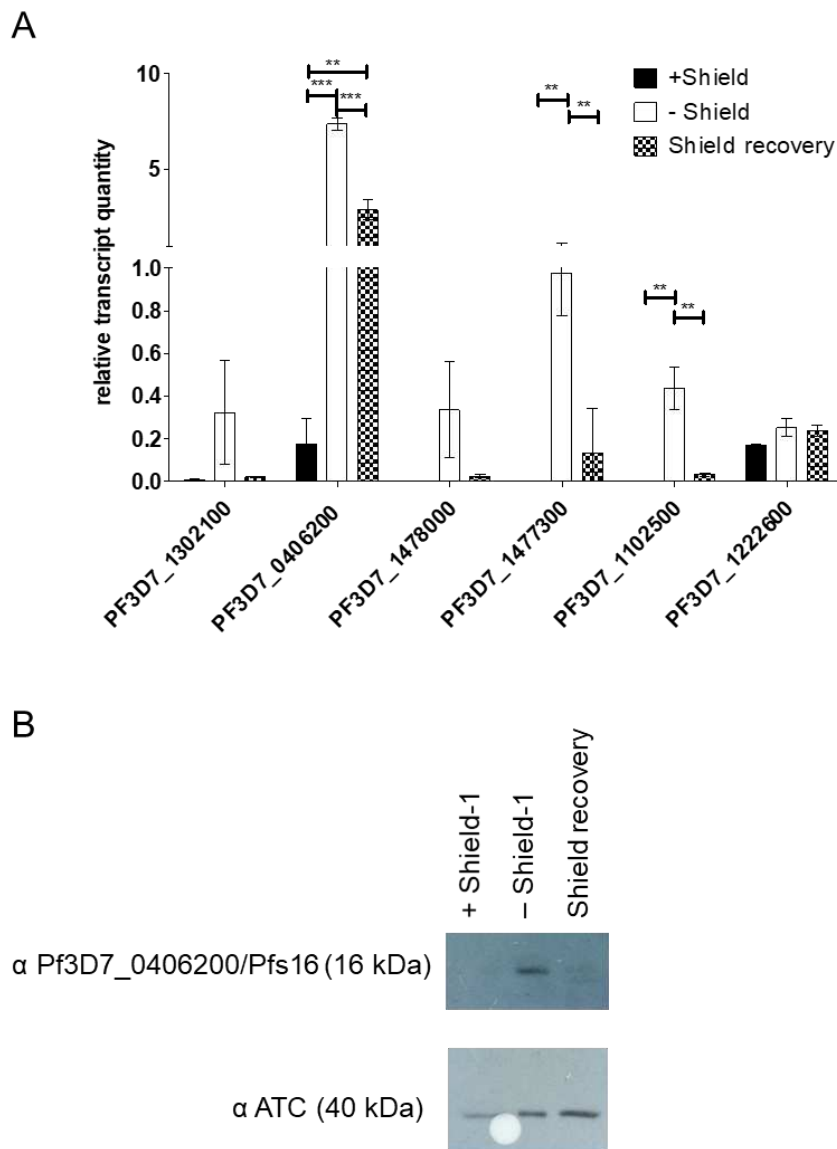


Figure 4: PfAP2-O-GFP-HA-DD24 is involved in the transcription/translation of gametocyte-related genes in *P. falciparum*. **A:** Transcript abundance of gametocyte-stage specific genes in PfAP2-O-GFP-HA-DD24 expressing, knocked-down (two reinvasions without Shield-1), and recovered parasites (two reinvasion cycles without Shield-1, followed by two reinvasion cycles in the presence of Shield-1). The data were normalized to seryl-tRNA ligase (PF3D7_0913900), used as the internal control. For statistical evaluation, the ANOVA test with Bonferroni's correction was used. “ ** ” is $p < 0.01$ and “ *** ” is $p < 0.005$. **B:** Western blot detecting Pfs16/Pf3D7_0406200 in extracts of NF54::PfAP2-O_GFP_HA_DD24 parasites in the three conditions (on Shield-1/knocked-down/recovered parasites). As a control, an antiATC antibody was used as before.

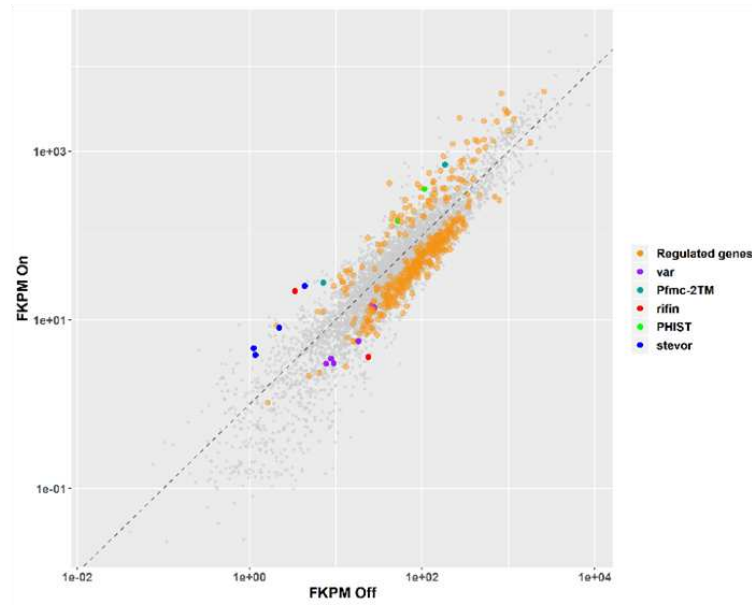
364

365

366

A

Figure 5



B

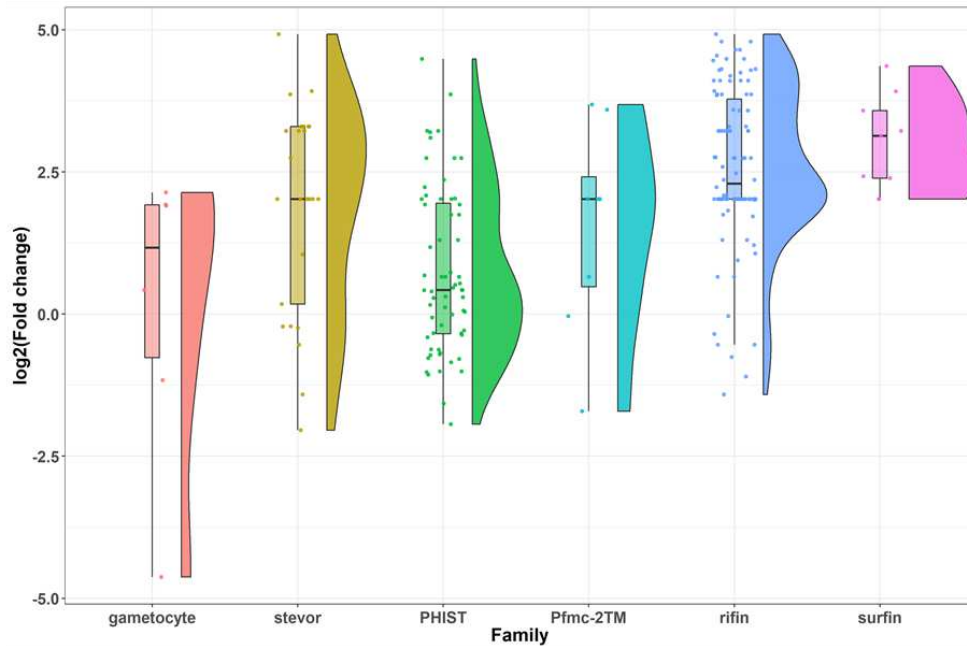
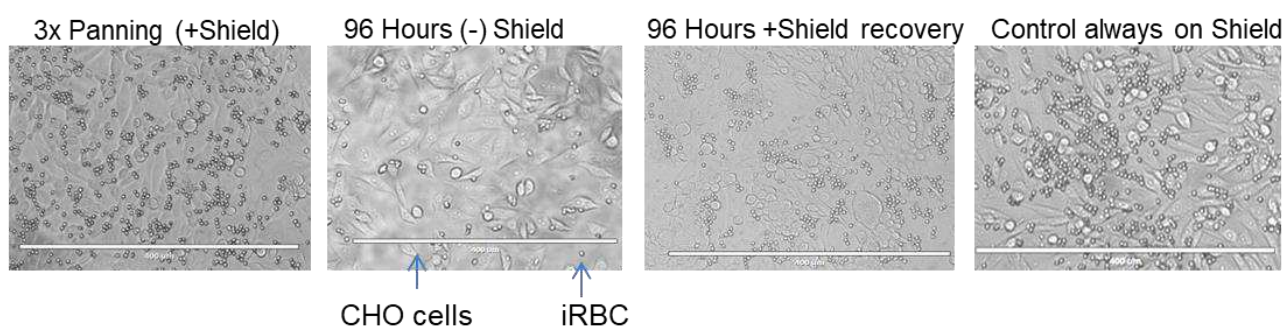


Figure 5: RNAseq analysis in PfAP2-O-GFP-HA-DD24 expressing or knocked down parasites in independent biological triplicates shows influence of PfAP2-O on variant gene transcripts. A: FPKM values in PfAP2-O-GFP-HA-DD24 + Shield-1 parasites “ON” (Y axis) versus PfAP2-O-GFP-HA-DD24 - Shield-1 Parasites “OFF” (X axis). Differentially expressed genes are shown in orange and genes where no significant changes were observed are in grey. Differentially expressed genes of multigenic families are highlighted in colours (Baggerley’s test with Bonferroni correction). Data are shown in log10 scale. **B:** Box/Whiskers and violin-plots of RNAseq results comparing indicated transcripts from PfAP2-O knocked-down and expressing parasites. Fold-change is shown in Log2 scale.

A



B

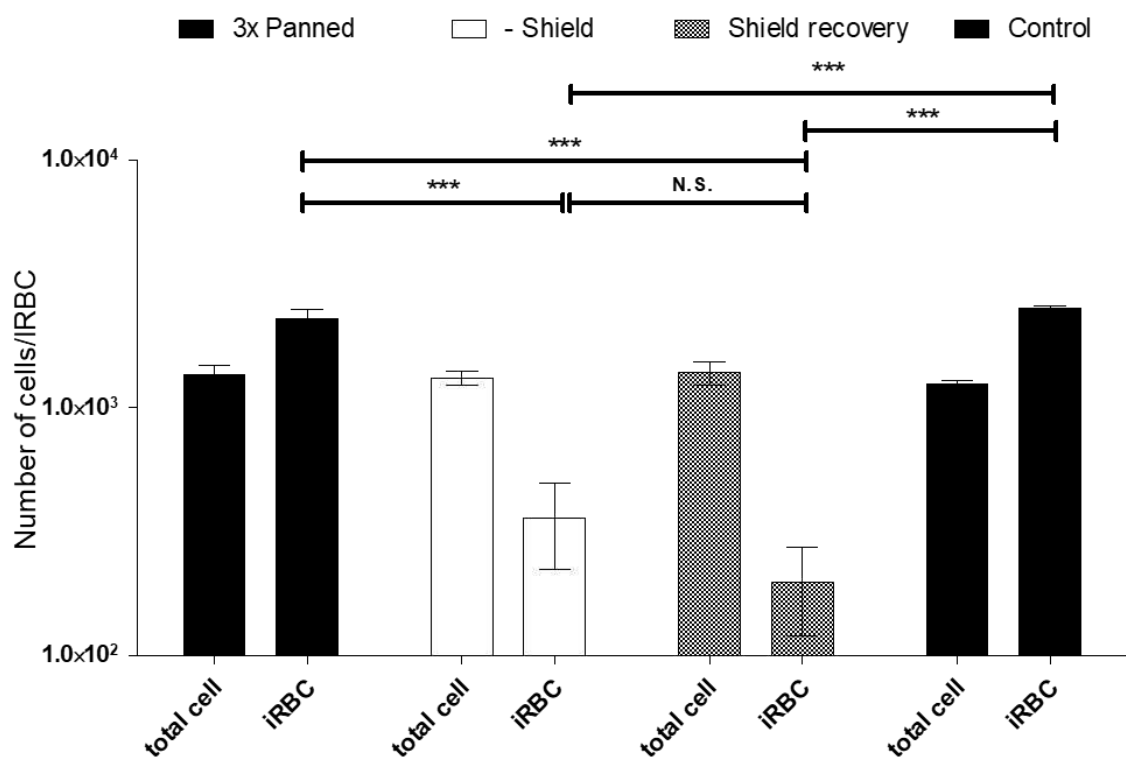


Figure 6. Adherent phenotype analysis shows decreased cytoadherence of iRBC during and after knockdown. A: Illustrative recording of each condition. The white bar at the bottom of each picture indicates 400 μ m. **B:** Graphic representation of three independent experiments. The significance of difference in numbers of adhering iRBC was calculated using Student's T-Test, and three asterisks indicate p values < 0.005. N.S. is not significant.

368

369

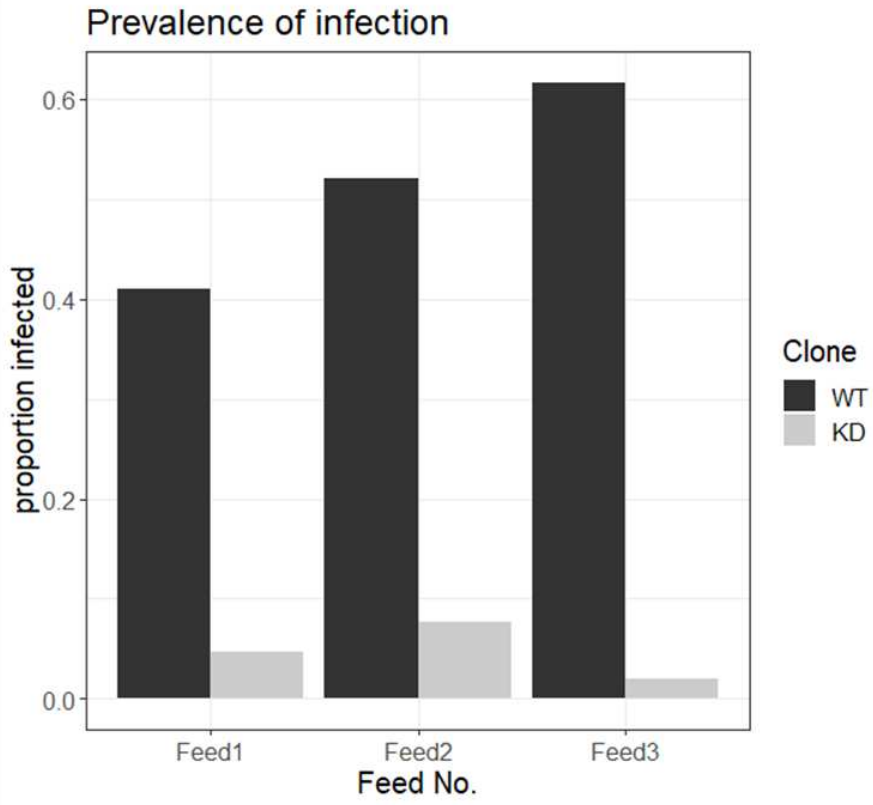
370

371

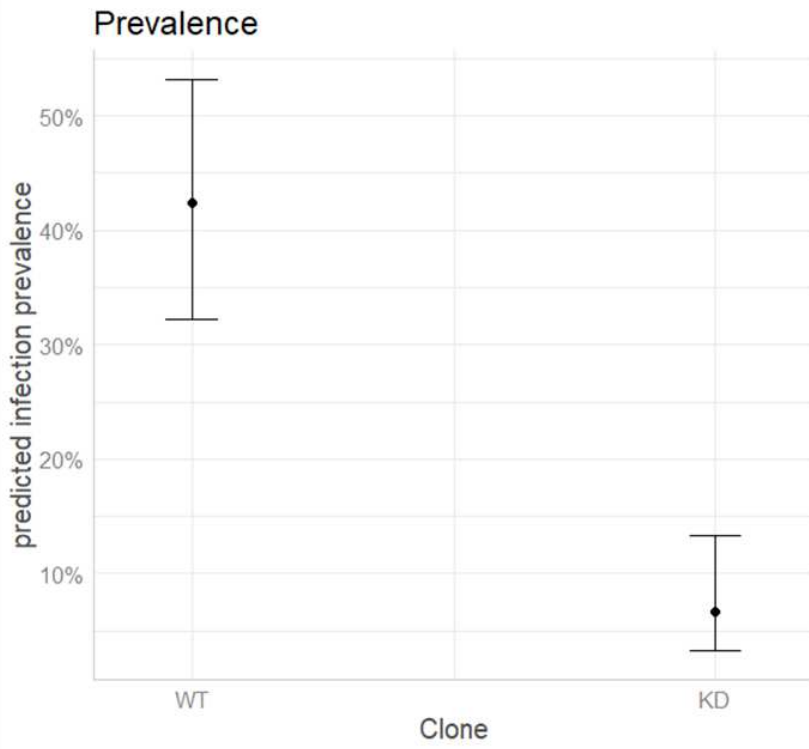
372

Figure 7

A



B



375 **Material and Methods**

376 *P. falciparum* culture

377 *P. falciparum* NF54 parasites and transgenic strains were cultured in 4 % hematocrit in RPMI
378 supplemented with 0.25 % Albumax 1 (Invitrogen)/5% human plasma under a 90% N₂, 5% CO₂, 5% O₂
379 atmosphere. Culture medium was changed daily or every two days and parasites were supplemented
380 with fresh blood every 4 days or more often depending on the parasitemia in the culture. The strains
381 containing a destabilizing domain were maintained in the presence of Shield-1 at 0.5 μM that stabilizes
382 the target protein ²⁷.

383 In order to obtain synchronized cultures, mature stage parasites were frequently (every 3
384 weeks) floated using Voluven 6% (Fresenius Kabi) using the method published by Lelievre and
385 colleagues ⁵². When purified ring stages were required, cultures with predominantly this form (up to 8
386 h after reinvasion) were treated for 10 min with 20 volumes of 5% sorbitol solution at room
387 temperature ⁵³.

388 **Molecular cloning/Plasmid construction**

389 *P. falciparum* knock-in expression plasmids were constructed using the PfAP2-O 3'-end
390 portion. This region was cloned into the transfection plasmid p_GFP_HA_DD24 (figure 1A). First,
391 genomic DNA (gDNA) was prepared from NF54 parasites using the Proteinase K/Phenol-Chloroform
392 method described in Methods in Malaria Research ⁵⁴. The final DNA pellet was resuspended in TE and
393 used as a template for PCR using oligonucleotide primers PfAP2-O fw: 5'-
394 AGATCTGAATTGTTCAGAACATTTAAATATAGTACC and PfAP2-O rev: 5'-
395 CTGCAGTAAATTATTAAGGGGGATGTTATTATTAAC (restriction sites BglIII and PstI underlined).

396 The oligonucleotides were used in standard PCRs (30 cycles of 94°C, 40 s, 50°C for 40 s and
397 65°C for 90 s, final polymerization of 10 min at 65°C). The PCR products were excised and purified via
398 the glassmilk method ⁵⁵, ligated into pGEM T easy (Promega) and transformed in DH10B chemically
399 competent *E. coli* cells. After plating and growth, colonies were grown in Terrific Broth - ampicillin (TB-
400 amp) supplemented liquid medium and the plasmids extracted using a standard miniprep protocol ⁵⁶.
401 Clones were sequenced by the dideoxy-dNTP method and checked for their integrity. The correct
402 fragment was subcloned in the p_GFP_HA_DD24 vector via PstI/BglIII. Recombinant plasmids used for
403 transfection were retransformed in *E. coli* SURE cells and grown in 200 ml TB-amp cultures of which
404 plasmids were recovered by the maxiprep protocol ⁵⁶.

405 **Transfection of blood stage parasites**

406 Empty erythrocytes were electroporated with 40 μg of maxiprep-purified plasmid in
407 incomplete cytomix following the Hasenkamp protocol ⁵⁷ with slight modifications. 2*10⁷ mature
408 parasites (schizonts) were concentrated up to 80% parasitemia and mixed with the electroporated

409 erythrocytes. After transfection, culture media were changed daily and parasites were submitted to
410 drug pressure with 2.5 nM WR99210 (a gift from Jacobus Inc, USA) 48 h after transfection. Transfected
411 parasites had their medium changed daily until day 6 when no more live parasites were visible. Once
412 parasites reappeared (normally 16-25 days after transfection) and ring stage parasitemia reached 3-4
413 %, several aliquots were frozen as backups. WR99210-resistant parasites were then cultivated for 20
414 days without WR99210 to promote the loss of episomal plasmids in parasites that did not recombine
415 in the target locus. Then, WR99210 was re-added until parasitemia increased again and new aliquots
416 were frozen. These drug on-off cycles were repeated for three times in order to enrich recombinant
417 parasites. Then, parasites were cloned by limiting dilution and DNA was analyzed in order to identify
418 clonal populations with the PfAP2-O locus modified using the oligonucleotides PfAP2-O “check” 5’-
419 CATCAAATGGATTTAATAATTGTTC and HA rev 5’-AGCGGCATAATCTGGAACATCGTAC.

420 **RNA purification and cDNA synthesis**

421 Total RNA was converted to cDNA following the protocol described in ²⁸. When parasitemias
422 reached 5%, RNA from parasites with and without Shield-1 treatment were harvested using Trizol (Life
423 Technologies) following the manufacturer’s instructions. The final RNA pellet resuspended in nuclease
424 free water. For reverse transcription, 10 µg of total RNA were digested three consecutive times by the
425 enzyme DNase I (Fermentas). The material obtained from this reaction was used for cDNA synthesis
426 using RevertAid reverse transcriptase (Fermentas) using random hexamer oligonucleotides (N₆).
427 Relative transcript quantities of different genes (see a list of oligos used for RT-PCR in Supplementary
428 Table 5) were then calculated by the 2^{-ΔCt} method ⁵⁸ using the seryl tRNA ligase transcript as
429 endogenous control.

430 **RNAseq with parasite-derived cDNA**

431 Total RNA was isolated from the harvested ring-stage parasites with Trizol reagent as described
432 above. The concentration of the isolated RNA was quantified using a Nanodrop device (Thermo
433 Scientific, USA) and the quality of the RNA was measured by a 2100 Bioanalyzer (Agilent Technologies,
434 CA). Then, the TruSeq RNA Sample Preparation Kit v2 low sample (LS) protocol (Illumina Inc., CA), was
435 used to construct cDNA libraries from 9 samples: 3 independent samples with Shield-1 (control), 3
436 independent samples without Shield-1 (knock down), and 3 independent samples after Shield-1 re-
437 addition (recovery). RNAseq was conducted in an Illumina NextSeq500 sequencer following the
438 recommendations of the provider using mid output flow cells and a total of 10 million reads per
439 sample. The CLC Genomics Workbench 7.01 program was used to remove the adapter and assess read
440 quality from the raw reads. The same platform was used to subject reads to the reference *P. falciparum*
441 genome available in the Ensemble Genome database (Release 26) and to generate gene read count
442 tables and FKPM values as well as to calculate the fold change of each gene (Supplementary Table 2).

443 The data visualization plots were obtained using R statistical software version 3.5.5 using the tidyverse
444 package version 1.2.1⁵⁹.

445 **Pull down of proteins associated with PF3D7_1143100_GFP_HA_DD24**

446 A total protein extract from the pPF3D7_1143100_GFP_HA_DD24 clone was prepared and the
447 protein complex containing the HA tag was purified using the HA-Tag (C29F4) Rabbit mAb (Sepharose
448 Beads conjugate, Cell Signaling Technology) kit. The obtained eluate was separated in a 12% SDS gel
449 using immunoprecipitated NF54 wild-type parasites as a control. To detect proteins in the precipitated
450 complex, the SDS gel was submitted to silver staining using the PlusOne Silver Staining Kit (GE
451 Healthcare, Supplementary figure 3). We observed three different protein bands in the extract from
452 the modified parasites compared to the negative control. These bands and bands corresponding to the
453 same size in the negative control were excised, trypsin-digested and analyzed by mass spectrometry.
454 Analyses were performed on LTQ-Orbitrap Velos ETD (Thermo) coupled with Easy nanoLC II (Thermo).
455 The peptides were separated on a C18RP column on a 95 min gradient. The instrumental conditions
456 were checked using 50 fmol of a tryptic digest of BSA as standard. The sample carryover was
457 completely removed between runs. The peptide search was conducted against the protein database
458 *Plasmodium falciparum*_reviewed Uniprot.

459 **Adherent phenotype selection of blood stage parasites in static assays (panning)**

460 The selection of adhesive phenotypes of infected red blood cells (IRBC) adherent to CHO-CD36
461 was done essentially as described in Gölnitz and colleagues²⁸. Briefly, Voluven-floated trophozoite
462 stage IRBC (5×10^7 - 10^8) were layered over confluent CHO-CD36 cells in RPMI/human plasma at pH6.8.
463 The IRBC were incubated over the cells for one hour at 37°C and gently mixed every 15 min. After 1 h,
464 the non-adherent IRBC were aspirated and the remaining adherent IRBC were washed three times with
465 RPMI at pH 6.8 and after the last washing step the number of adherent IRBC was documented. The
466 remaining IRBC were then detached using RPMI/plasma at pH 7.2-7.4 and returned to the normal
467 culture conditions. The process was repeated 3 times after which strongly adherent IRBC
468 predominantly expressing *var* gene PF3D7_0412400 (CHO-CD36 binding) were obtained. For the
469 silencing assay, cells were grown in 6well plates and central areas were marked in each well. For the
470 cytoadherence readout, ten pictures for each condition were taken using the EVOS FL digital inverted
471 microscope (AMG). The CHO cells and parasites were counted and the results were plotted using
472 GraphPad Prism 5 software.

473

474 **Fluorescence Microscopy**

475 For GFP expression analysis, parasites were fixed as described in⁶⁰ followed by incubation with
476 PBS/Saponin 0.01% and DAPI at a final concentration of 2 µg/mL at 37°C for 1 h. After that, the

477 parasites were washed 3 times with PBS/Saponin 0.01% and incubated with the membrane marker
478 Wheat Germ agglutinin (WGA) Texas Red™-X conjugate (Invitrogen) in PBS/Saponin 0.01% for 20
479 minutes at 37°C. Finally, parasites were washed three times with PBS/Saponin. Images were acquired
480 in a fluorescence microscope Zeiss Axio Observer Z1 and processed using Photoshop version 5.

481 **Western blot**

482 Total protein extract was obtained from saponin-lysed parasites, separated in 10% SDS
483 polyacrylamide gels and transferred to a Hybond C nitrocellulose membrane (GE Healthcare). After
484 blocking with 4% nonfat milk in 1xPBS/0.1% Tween20, membranes were incubated with a murine
485 antiHA antibody (Sigma-Aldrich, 1:1000) or anti-Pfs16 followed by an antiMouse IgG-peroxydase
486 antibody (KPL, 1:5000) incubation. Blots were washed with PBS/Tween between incubations and
487 finally incubated with WesternPico Super signal substrate (Pierce/Thermo) for detection. As a loading
488 control, a murine polyclonal antiATC antibody (1:1000) was used. The signal intensities were measured
489 using the ImageJ program (NIH).

490 **Mosquito infection with *P. falciparum* gametocytes**

491 *Plasmodium falciparum* wild type (NF54) and transgenic parasites were maintained under standard
492 conditions to produce infectious gametocytes as described ⁶¹ in the absence of Shield-1. For each
493 parasite line, 100 mosquitoes of *An. coluzzii* Ngousso strain were infected using membrane feeding ⁶²,
494 unfed mosquitoes were removed and the blood fed mosquitoes were maintained under standard
495 insectary conditions (26 ± 1 °C, 80% humidity, 12 h light:12 h dark cycle) and fed ad libitum on 5%
496 glucose solution containing 0.05% (w/v) 4-aminobenzoic acid (PABA). Mosquitoes were dissected 10
497 days post-infection and the midguts were examined microscopically (400x magnification) for the
498 presence and number of oocysts. Permission for the non-therapeutic use of human blood was obtained
499 from the Scottish National Blood Transfusion Service Committee for the Governance of Blood and
500 Tissue Samples for Non-Therapeutic Use, reference 18-15.

501 **Statistical analysis of mosquito infection**

502 To estimate the effect of the PfApiAP2-Sp and PfApiAP2-O knockout/knockdown in *P. falciparum*
503 transmission, a generalized linear mixed-effect model GLMM was employed using the package lme4 ⁶³
504 in R software version 3.5.3 ⁶⁴. To assess the effect on infection prevalence, a binomial GLMM with log
505 link was used with fixed variables of parasite clone and gametocyte number present in the bloodmeal,
506 with the replicate (infectious feed number) included as a random effect. A stepwise backward selection
507 was used to identify the significant fixed effects ⁶⁵, with optimal model selection performed using the
508 Akaike Information Criterion (AIC) for which lower scores indicate better model fits, and with likelihood
509 ratio tests were used to compare the different models. Model diagnostics, including normality of
510 residuals were done by visual inspection of residuals versus fitted values for each random effect group,

511 and a Shapiro-Wilk test. Finally, to calculate how much of the variance was explained by the variables
512 included in the final model, an R squared for the generalized linear mixed effect model `r2glmm`⁶⁶, was
513 applied. For this, the package `MuMIn`, version 1.41.0 was used, and the `R2m` indicates the variation in
514 prevalence explained by the fixed effects and the `R2c` included all the variables used in the model.

515 For intensity of infection (model 2), a zero-inflated negative binomial distribution was fitted to
516 the data in a GLMM analysis using the package `glmmTMB`⁶⁷, with the family `nbinom 2` (log link). The
517 final minimum model included fixed variables of clone and the number of gametocytes present in the
518 bloodmeal, with feed number as a random effect: For model selection, diagnostics and to test
519 overdispersion the same procedures from model 1 were used. As above, R software version 3.5.3⁶⁸
520 was used for data analysis and models fit, as additional packages were used `lme4`⁶³, `DHARMA` 0.3.0
521 `aods3`⁷⁰ and `MuMIn` (v1.42.5)⁶⁶.

522 Acknowledgments

523 The authors would like to thank Professor Giuseppe Palmisano from University of São Paulo
524 for assistance with the mass spectrometry analysis. Wolfgang Fischer for technical support in
525 University of São Paulo laboratories and Dorothy Armstrong and Elizabeth Peat for the maintenance
526 of the IBAHCM/Glasgow University mosquito insectaries.

527

528 Literature cited

- 529 1. World Health Organization. *World Malaria Report 2019*. Geneva. (2019).
- 530 2. Dondorp, A. M. *et al.* Artemisinin Resistance in Plasmodium falciparum Malaria. *n engl j med*
531 *Mae Sot Fam. Heal. Int. Churchill Hosp. N.J.W. N Engl J Med* **361**, 455–67 (2009).
- 532 3. WHO | Insecticide resistance. *WHO* (2020).
- 533 4. Delves, M. J., Angrisano, F. & Blagborough, A. M. Antimalarial Transmission-Blocking
534 Interventions: Past, Present, and Future. *Trends Parasitol.* **34**, 735–746 (2018).
- 535 5. Su, X. Z. *et al.* The large diverse gene family *var* encodes proteins involved in cytoadherence
536 and antigenic variation of Plasmodium falciparum-infected erythrocytes. *Cell* **82**, 89–100
537 (1995).
- 538 6. Scherf, A. *et al.* Antigenic variation in malaria: in situ switching, relaxed and mutually exclusive
539 transcription of *var* genes during intra-erythrocytic development in Plasmodium falciparum.
540 *EMBO J* **17**, 5418–5426 (1998).

- 541 7. Chen, Q. *et al.* Developmental selection of var gene expression in Plasmodium falciparum.
542 *Nature* **394**, 392–395 (1998).
- 543 8. Brancucci, N. M. B., Witmer, K., Schmid, C. D., Flueck, C. & Voss, T. S. Identification of a cis-
544 acting DNA-protein interaction implicated in singular var gene choice in Plasmodium
545 falciparum. *Cell. Microbiol.* **14**, 1836–1848 (2012).
- 546 9. Amit-Avraham, I. *et al.* Antisense long noncoding RNAs regulate var gene activation in the
547 malaria parasite Plasmodium falciparum. *Proc. Natl. Acad. Sci. U. S. A.* **112**, 982–991 (2015).
- 548 10. Jing, Q. *et al.* Plasmodium falciparum var Gene Is Activated by Its Antisense Long Noncoding
549 RNA. *Front. Microbiol.* **9**, (2018).
- 550 11. Voss, T. S. *et al.* A var gene promoter controls allelic exclusion of virulence genes in
551 Plasmodium falciparum malaria. *Nature* **439**, 1004–1008 (2006).
- 552 12. Guizetti, J., Barcons-Simon, A. & Scherf, A. Trans-acting GC-rich non-coding RNA at var
553 expression site modulates gene counting in malaria parasite. *Nucleic Acids Res.* gkw664
554 (2016). doi:10.1093/nar/gkw664
- 555 13. Barcons-Simon, A., Cordon-Obras, C., Guizetti, J., Bryant, J. M. & Scherf, A. CRISPR
556 Interference of a Clonally Variant GC-Rich Noncoding RNA Family Leads to General Repression
557 of var Genes in Plasmodium falciparum. *MBio* **11**, (2020).
- 558 14. Fan, Y. *et al.* Rrp6 Regulates Heterochromatic Gene Silencing via ncRNA RUF6 Decay in Malaria
559 Parasites. *MBio* **11**, e01110-20 (2020).
- 560 15. Brancucci, N. M. B. *et al.* Heterochromatin Protein 1 Secures Survival and Transmission of
561 Malaria Parasites. *Cell Host Microbe* **16**, 165–176 (2014).
- 562 16. Pérez-Toledo, K. *et al.* Plasmodium falciparum heterochromatin protein 1 binds to tri-
563 methylated histone 3 lysine 9 and is linked to mutually exclusive expression of var genes.
564 *Nucleic Acids Res.* **37**, 2596–606 (2009).
- 565 17. Li, Z. *et al.* DNA helicase RecQ1 regulates mutually exclusive expression of virulence genes in
566 Plasmodium falciparum via heterochromatin alteration. *Proc. Natl. Acad. Sci. U. S. A.* **116**,
567 3177–3182 (2019).
- 568 18. Lavstsen, T., Salanti, A., Jensen, A. T. R., Arnot, D. E. & Theander, T. G. Sub-grouping of
569 Plasmodium falciparum 3D7 var genes based on sequence analysis of coding and non-coding
570 regions. *Malar. J.* **2**, 27 (2003).

- 571 19. Zhang, Q. *et al.* Exonuclease-mediated degradation of nascent RNA silences genes linked to
572 severe malaria. *Nature* **513**, 431–5 (2014).
- 573 20. Yuda, M., Iwanaga, S., Shigenobu, S., Kato, T. & Kaneko, I. Transcription factor AP2-Sp and its
574 target genes in malarial sporozoites. *Mol. Microbiol.* **75**, 854–63 (2010).
- 575 21. Yuda, M. *et al.* Identification of a transcription factor in the mosquito-invasive stage of malaria
576 parasites. *Mol. Microbiol.* **71**, 1402–14 (2009).
- 577 22. Kafsack, B. F. C. *et al.* A transcriptional switch underlies commitment to sexual development in
578 malaria parasites. *Nature* **507**, 248–252 (2014).
- 579 23. Balaji, S., Babu, M. M., Iyer, L. M. & Aravind, L. Discovery of the principal specific transcription
580 factors of Apicomplexa and their implication for the evolution of the AP2-integrase DNA
581 binding domains. *Nucleic Acids Res.* **33**, 3994–4006 (2005).
- 582 24. Campbell, T. L., De Silva, E. K., Olszewski, K. L., Elemento, O. & Llinás, M. Identification and
583 genome-wide prediction of DNA binding specificities for the ApiAP2 family of regulators from
584 the malaria parasite. *PLoS Pathog.* **6**, e1001165 (2010).
- 585 25. Flueck, C. *et al.* A major role for the Plasmodium falciparum ApiAP2 protein PfSIP2 in
586 chromosome end biology. *PLoS Pathog.* **6**, e1000784 (2010).
- 587 26. Martins, R. M. *et al.* An ApiAP2 member regulates expression of clonally variant genes of the
588 human malaria parasite Plasmodium falciparum. *Sci. Rep.* **7**, 14042 (2017).
- 589 27. de Azevedo, M. F. M. F. M. F. *et al.* Systematic Analysis of FKBP Inducible Degradation Domain
590 Tagging Strategies for the Human Malaria Parasite Plasmodium falciparum. *PLoS One* **7**,
591 e40981 (2012).
- 592 28. Gölnitz, U., Albrecht, L. & Wunderlich, G. Var transcription profiling of Plasmodium falciparum
593 3D7: assignment of cytoadherent phenotypes to dominant transcripts. *Malar. J.* **7**, 14 (2008).
- 594 29. Lopez-Rubio, J. J. *et al.* 5' flanking region of var genes nucleate histone modification patterns
595 linked to phenotypic inheritance of virulence traits in malaria parasites. *Mol. Microbiol.* **66**,
596 1296–305 (2007).
- 597 30. Yuda, M., Iwanaga, S., Kaneko, I. & Kato, T. Global transcriptional repression: An initial and
598 essential step for Plasmodium sexual development. *Proc. Natl. Acad. Sci. U. S. A.* **112**, 12824–9
599 (2015).

- 600 31. Iwanaga, S., Kaneko, I., Kato, T. & Yuda, M. Identification of an AP2-family Protein That Is
601 Critical for Malaria Liver Stage Development. *PLoS One* **7**, e47557 (2012).
- 602 32. Santos, J. M. *et al.* Red Blood Cell Invasion by the Malaria Parasite Is Coordinated by the
603 PfAP2-I Transcription Factor. *Cell Host Microbe* **21**, 731-741.e10 (2017).
- 604 33. Tonkin, C. J. *et al.* Sir2 paralogue cooperate to regulate virulence genes and antigenic
605 variation in *Plasmodium falciparum*. *PLoS Biol.* **7**, e84 (2009).
- 606 34. Guizetti, J. & Scherf, A. Silence, activate, poise and switch! Mechanisms of antigenic variation
607 in *Plasmodium falciparum*. *Cell. Microbiol.* **15**, 718–26 (2013).
- 608 35. Epp, C., Li, F., Howitt, C. A., Chookajorn, T. & Deitsch, K. W. Chromatin associated sense and
609 antisense noncoding RNAs are transcribed from the var gene family of virulence genes of the
610 malaria parasite *Plasmodium falciparum*. *RNA* **15**, 116–27 (2009).
- 611 36. Freitas-Junior, L. H. *et al.* Telomeric heterochromatin propagation and histone acetylation
612 control mutually exclusive expression of antigenic variation genes in malaria parasites. in *Cell*
613 **121**, 25–36 (2005).
- 614 37. Oehring, S. C. *et al.* Organellar proteomics reveals hundreds of novel nuclear proteins in the
615 malaria parasite *Plasmodium falciparum*. *Genome Biol.* **13**, R108 (2012).
- 616 38. Chookajorn, T. *et al.* Epigenetic memory at malaria virulence genes. in *Proc Natl Acad Sci U S A*
617 **104**, 899–902 (2007).
- 618 39. Salcedo-Amaya, A. M. *et al.* Dynamic histone H3 epigenome marking during the
619 intraerythrocytic cycle of *Plasmodium falciparum*. *Proc Natl Acad Sci U S A* **106**, 9655–9660
620 (2009).
- 621 40. Andrews, K. T., Adams, Y., Viebig, N. K., Lanzer, M. & Schwartz-Albiez, R. Adherence of
622 *Plasmodium falciparum* infected erythrocytes to CHO-745 cells and inhibition of binding by
623 protein A in the presence of human serum. *Int. J. Parasitol.* **35**, 1127–34 (2005).
- 624 41. Hsieh, F.-L. *et al.* The structural basis for CD36 binding by the malaria parasite. *Nat. Commun.*
625 **7**, 12837 (2016).
- 626 42. Lavstsen, T. *et al.* PNAS Plus: *Plasmodium falciparum* erythrocyte membrane protein 1 domain
627 cassettes 8 and 13 are associated with severe malaria in children. *Proc. Natl. Acad. Sci.* **109**,
628 1791–1800 (2012).

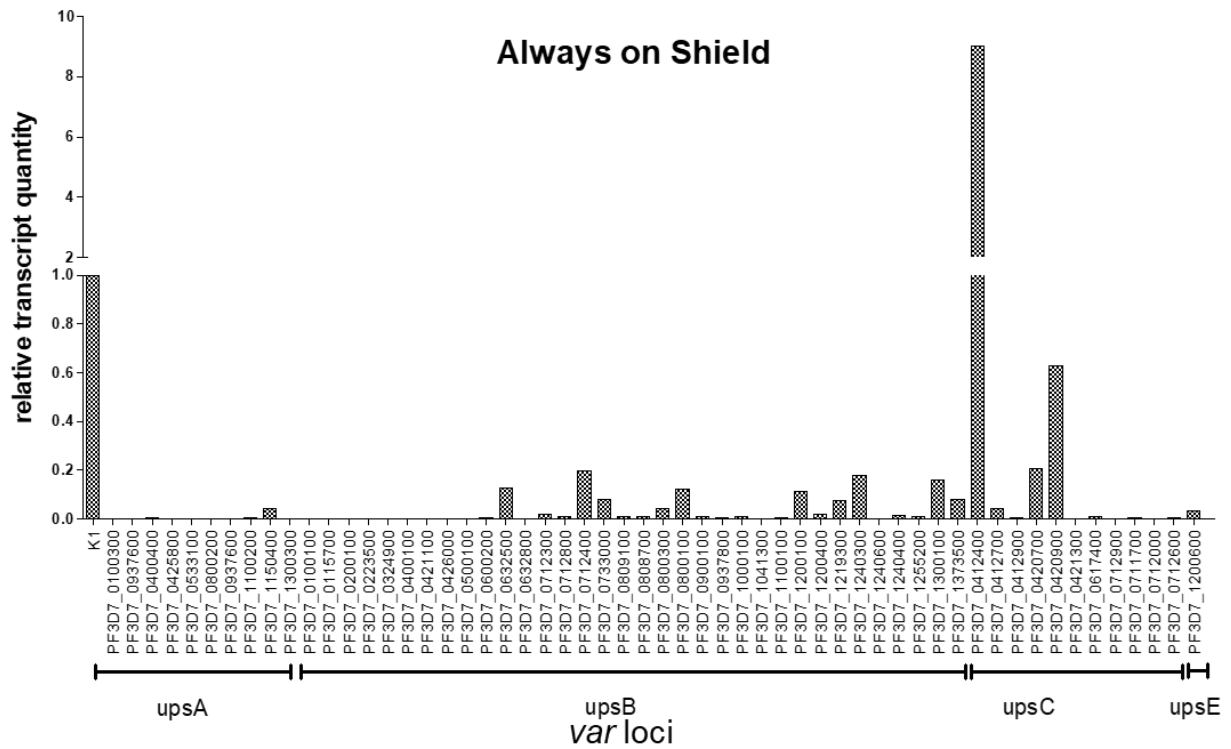
- 629 43. Warimwe, G. M. *et al.* Plasmodium falciparum var gene expression is modified by host
630 immunity. *Proc. Natl. Acad. Sci. U. S. A.* **106**, 21801–6 (2009).
- 631 44. Lavstsen, T. *et al.* Expression of Plasmodium falciparum erythrocyte membrane protein 1 in
632 experimentally infected humans. *Malar. J.* **4**, 21 (2005).
- 633 45. Mustaffa, K. M. F., Storm, J., Whittaker, M., Szestak, T. & Craig, A. G. In vitro inhibition and
634 reversal of Plasmodium falciparum cytoadherence to endothelium by monoclonal antibodies
635 to ICAM-1 and CD36. *Malar. J.* **16**, 279 (2017).
- 636 46. Jiang, L. *et al.* PfSETvs methylation of histone H3K36 represses virulence genes in Plasmodium
637 falciparum. *Nature* **499**, 223–7 (2013).
- 638 47. Dechering, K. J., Thompson, J., Dodemont, H. J., Eling, W. & Konings, R. N. . Developmentally
639 regulated expression of pfs16, a marker for sexual differentiation of the human malaria
640 parasite Plasmodium falciparum. *Mol. Biochem. Parasitol.* **89**, 235–244 (1997).
- 641 48. Mair, G. R. *et al.* Regulation of sexual development of Plasmodium by translational repression.
642 *Science (80-.)*. **313**, 667–9 (2006).
- 643 49. Sinha, A. *et al.* A cascade of DNA-binding proteins for sexual commitment and development in
644 Plasmodium. *Nature* **507**, 253–7 (2014).
- 645 50. Filarsky, M. *et al.* GDV1 induces sexual commitment of malaria parasites by antagonizing HP1-
646 dependent gene silencing. *Science (80-.)*. **359**, 1259–1263 (2018).
- 647 51. Modrzynska, K. *et al.* A Knockout Screen of ApiAP2 Genes Reveals Networks of Interacting
648 Transcriptional Regulators Controlling the Plasmodium Life Cycle. *Cell Host Microbe* **21**, 11–22
649 (2017).
- 650 52. Lelièvre, J. *et al.* An alternative method for Plasmodium culture synchronization. *Exp Parasitol*
651 **109**, 195–197 (2005).
- 652 53. Lambros, C. & Vanderberg, J. P. Synchronization of Plasmodium falciparum erythrocytic stages
653 in culture. *J Parasitol* **65**, 418–420 (1979).
- 654 54. Ljungström, I., Perlmann, H., Schlichtherle, M., Scherf, A. & Wahlgren, M. *Methods in Malaria*
655 *Research*. (MR4/ATCC, BioMalPar, 2008).
- 656 55. Boyle, J. S. & Lew, A. M. An inexpensive alternative to glassmilk for DNA purification. *Trends*
657 *Genet* **11**, 8 (1995).

- 658 56. Sambrook, J., G. M. [Molecular Cloning: A Laboratory Manual. 4 ed. Cold Spring Harbor
659 Laboratory Press 1, (2012).
- 660 57. Hasenkamp, S., Russell, K. T. & Horrocks, P. Comparison of the absolute and relative
661 efficiencies of electroporation-based transfection protocols for Plasmodium falciparum.
662 *Malar. J.* **11**, 210 (2012).
- 663 58. Livak, K. J. & Schmittgen, T. D. Analysis of Relative Gene Expression Data Using Real-Time
664 Quantitative PCR and the $2^{-\Delta\Delta CT}$ Method. *Methods* **25**, 402–408 (2001).
- 665 59. Wickham, H. tidyverse: Easily Install and Load the ‘Tidyverse’. R package version 1.2.1.
666 <https://CRAN.R-project.org/package=tidyverse>. (2017).
- 667 60. Tonkin, C. J. *et al.* Localization of organellar proteins in Plasmodium falciparum using a novel
668 set of transfection vectors and a new immunofluorescence fixation method. *Mol. Biochem.*
669 *Parasitol.* **137**, 13–21 (2004).
- 670 61. Hyde, J. E., Carter, R., Ranford-Cartwright, L. & Alano, P. The Culture and Preparation of
671 Gametocytes of Plasmodium falciparum for Immunochemical, Molecular, and Mosquito
672 Infectivity Studies. *Protoc. Mol. Parasitol.* **27**, 67–88 (2003).
- 673 62. Ranford-Cartwright, L. C. *et al.* Characterisation of Species and Diversity of Anopheles
674 gambiae Keele Colony. *PLoS One* **11**, e0168999 (2016).
- 675 63. Bates, D., Mächler, M., Bolker, B. M. & Walker, S. C. Fitting linear mixed-effects models using
676 lme4. *J. Stat. Softw.* **67**, 1–48 (2015).
- 677 64. Team, R. C. R: A Language and Environment for Statistical Computing. (2013).
- 678 65. Burnham, K. & Anderson, D. *Model Selection and Multimodel Inference: A Practical*
679 *Information-Theoretic Approach*. (Springer Verlag, 2002).
- 680 66. Nakagawa, S., Johnson, P. C. D. & Schielzeth, H. The coefficient of determination R^2 and intra-
681 class correlation coefficient from generalized linear mixed-effects models revisited and
682 expanded. *J. R. Soc. Interface* **14**, 20170213 (2017).
- 683 67. Brooks, M. E. *et al.* glmmTMB balances speed and flexibility among packages for zero-inflated
684 generalized linear mixed modeling. *R J.* **9**, 378–400 (2017).
- 685 68. R: The R Project for Statistical Computing.
- 686 69. DHARMA: residual diagnostics for hierarchical (multi-level/mixed) regression models.

687 70. Lesnoff, M., Fr>, <matthieu Lesnoff@cirad, Lancelot, R. & Lancelot, M. R. *Package 'aods3' Title*
 688 *Analysis of Overdispersed Data using S3 Methods.* (2018).

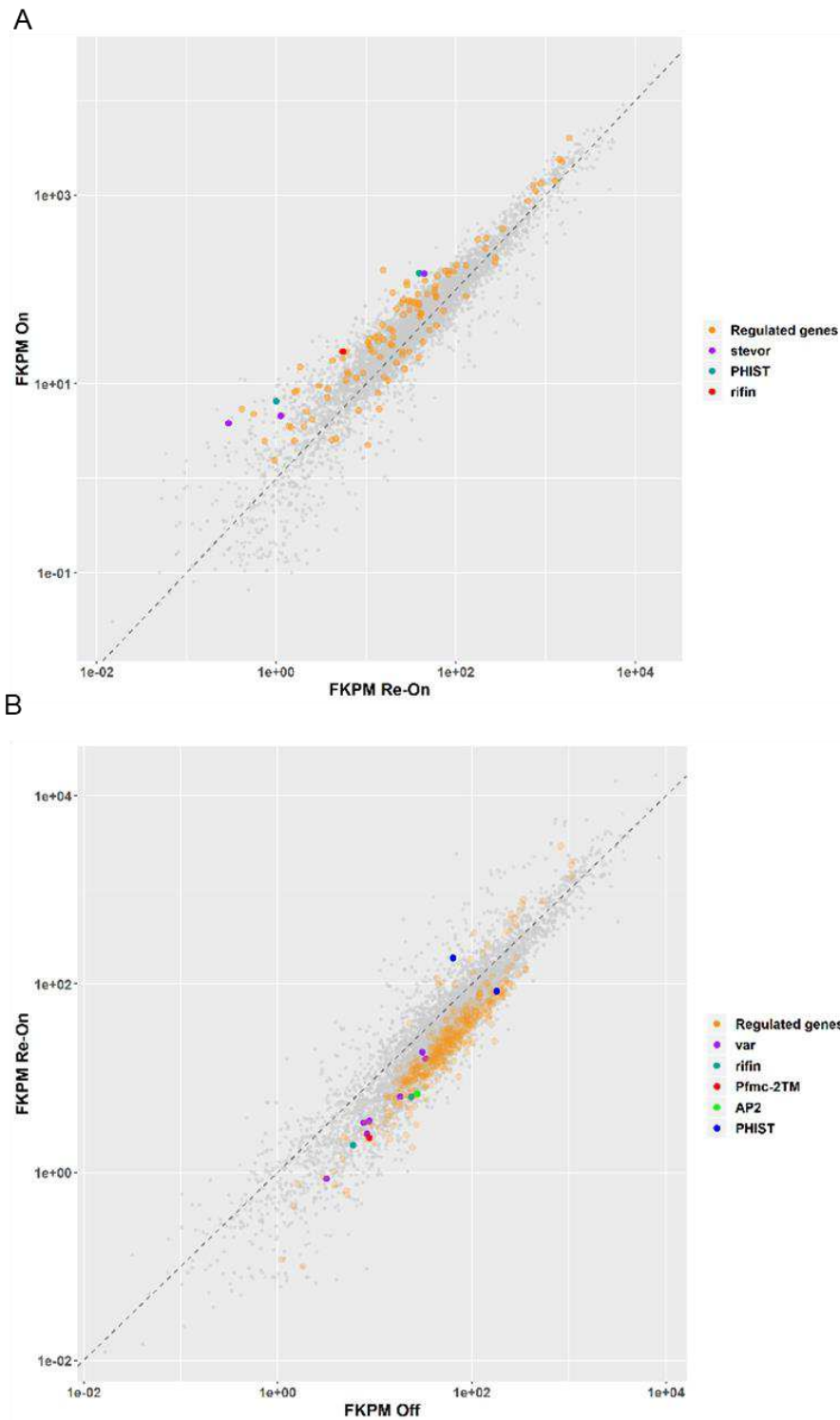
689 **Supplementary figure**

690



Supplementary figure 1: *var* transcription profile in parasites never submitted to silencing of PfAP2-O (Always on Shield-1, at the end of the knockdown experiment), measured by RT-qPCR as described. K1 is the transcript of t-seryl ligase, used as an internal control (see Methods for details).

691

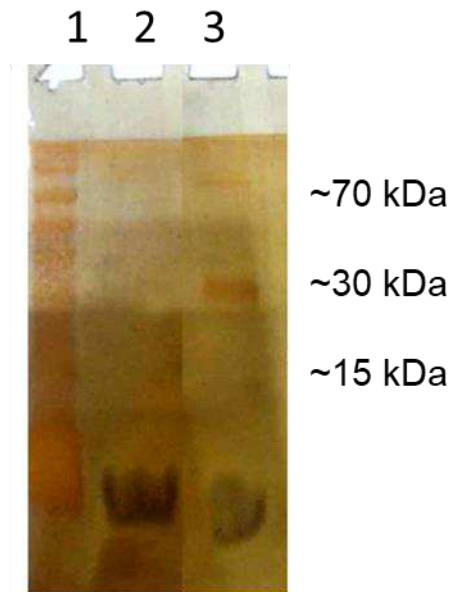


Supplementary figure 2. RNA seq analysis in PfAP2-O expressing and knocked-down parasites in biological triplicates **A:** FPKM values in PfAP2-0 + Shield parasites “ON”(Y axis) and PfAP2-O (-) Shield Parasites “OFF” (X axis). The differentially expressed genes are in orange and genes were no statistically significant changes were observed are in grey. Differentially expressed genes of multigenic families are highlighted in colours (Baggerley’s test with Bonferroni correction).

692

693

694

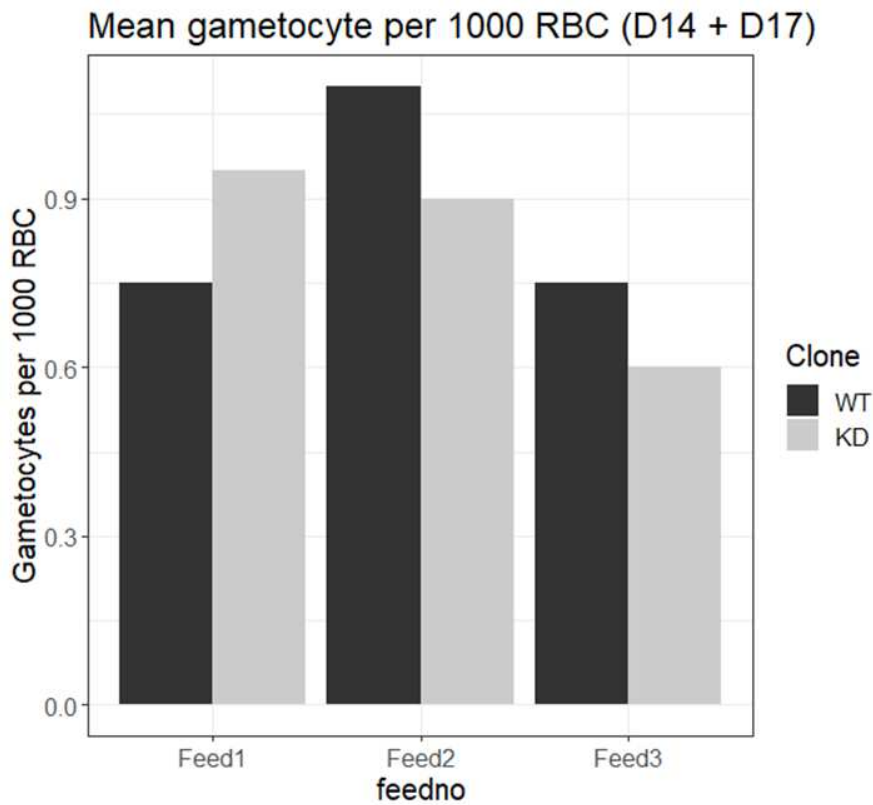


Supplementary figure 3. Silver staining of purified protein complexes after antiHA immunoprecipitation. Bands in the size of 70 kDa, 30 kDa and 15 kDa were excised from Coomassie colloidal blue stained gels run in parallel and analyzed by mass spectrometry. Lane 1 represents the molecular weight, lane 2 is the immunoprecipitated NF54 wild type extract and lane 3 the immunoprecipitated protein extract from the PfAP2-O_GFP_HA_DD24 strain. See Methods for details.

695

696

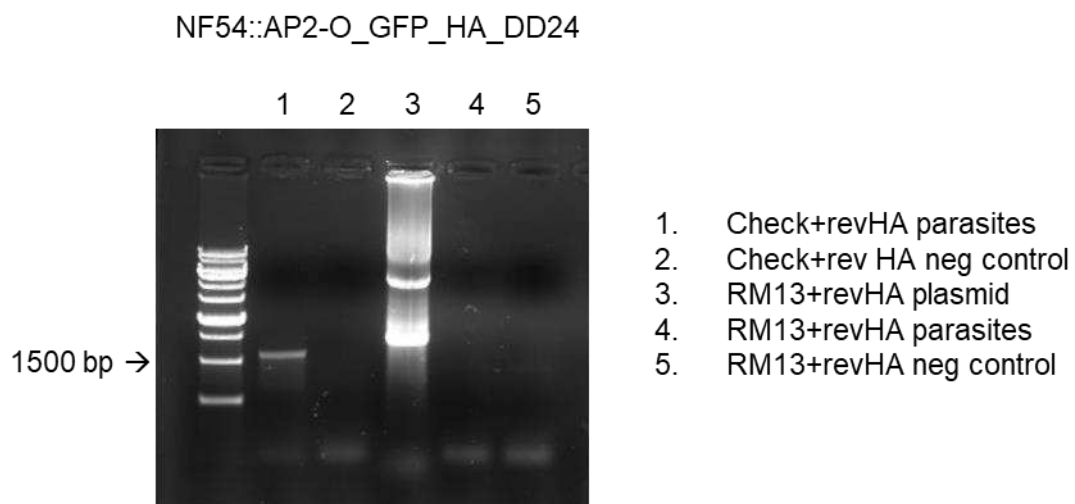
697



Supplementary figure 4. Mean gametocytes number per 1000 RBC counted for each clone in three independent experiment for *Anopheles coluzzzi* infection.

698

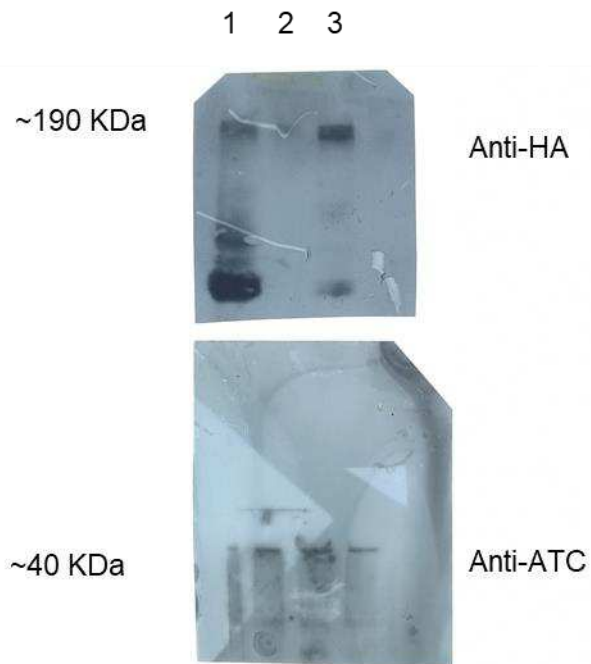
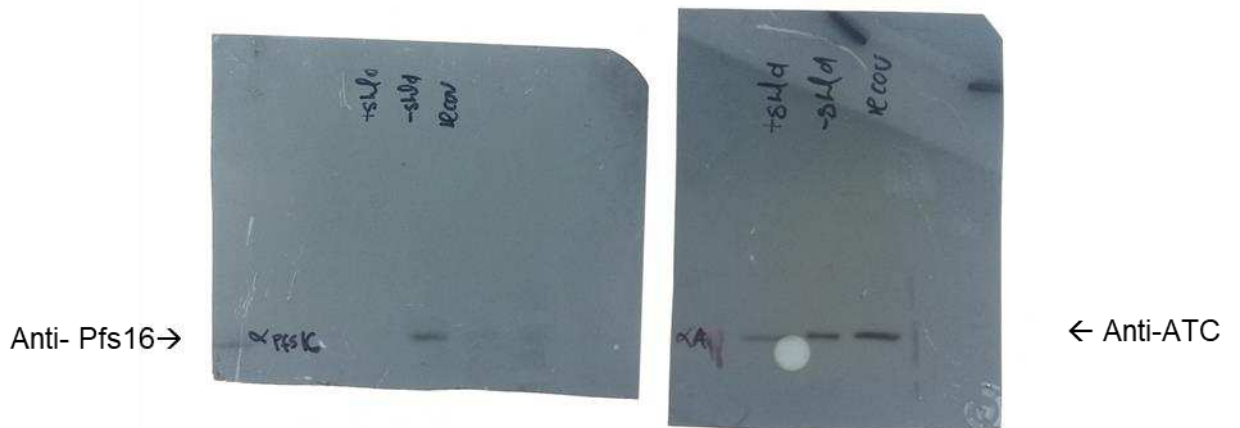
Original pictures/X ray films from Figures 1 and 4



Supplementary figure 4. Original Agarose gel image from the PCR reaction of Figure 1, showing integration of the plasmid in the Pf3D7_1143100 locus.

699

700

A**B**

Supplementary figure 5. Original images from western blot results shown in figure 1 and 4. **A:** Original Western blot from figure 1C. Lane 1: Parasites grown in the presence of Shield-1, Lane 2: Parasites grown for two reinvasions without Shield-1, lane 3: Parasites after reestablishment of PfAP2-O-GFP-DD24 by re-addition of Shield-1 for two reinvasion cycles.

B: Original western blot from Figure 4B. Left: Anti Pfs 16. Right: Anti-ATC. See Methods for details.

Figures

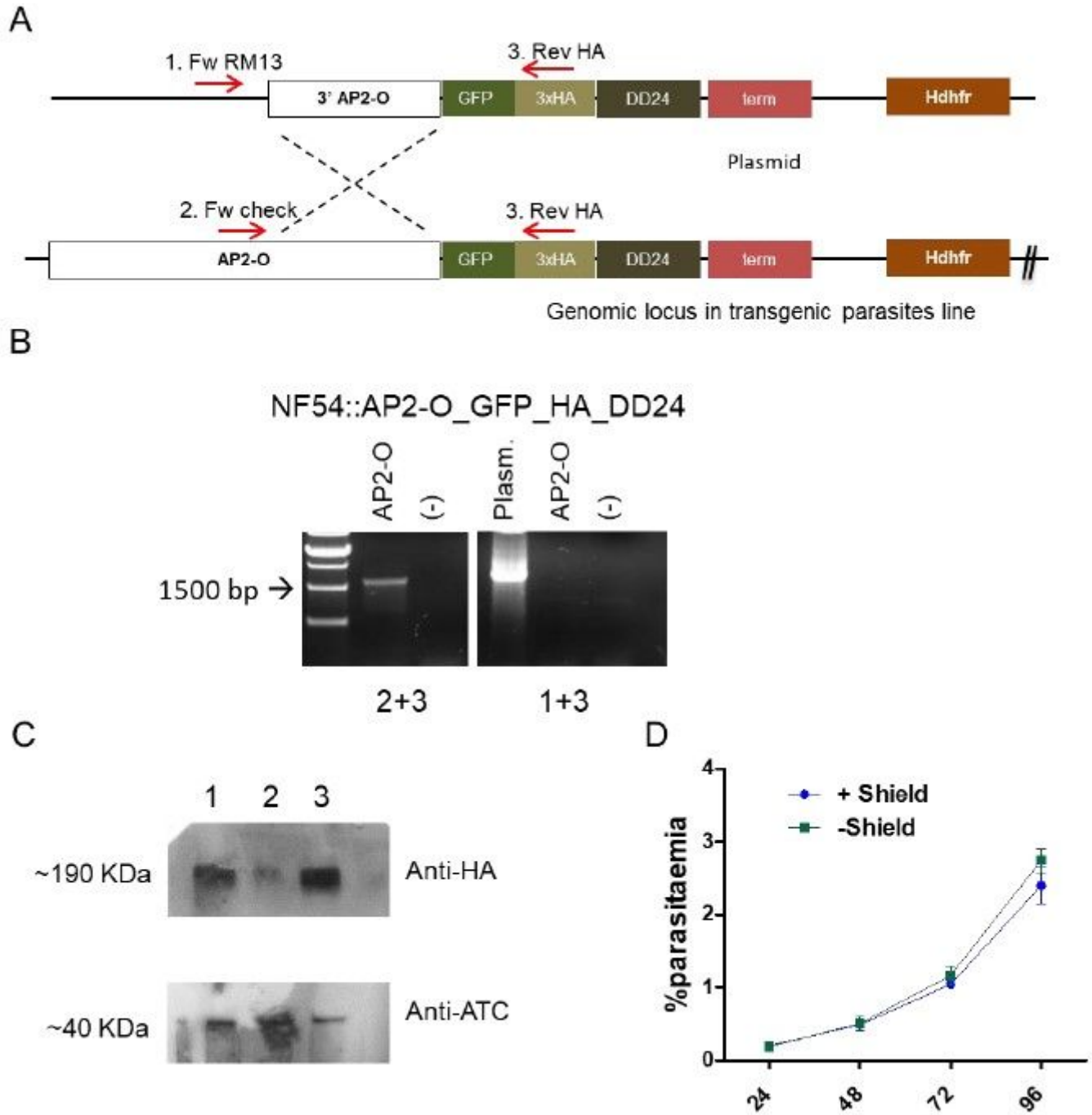


Figure 1

PfAP2-O modification and subsequent knockdown leads to no discernible modification

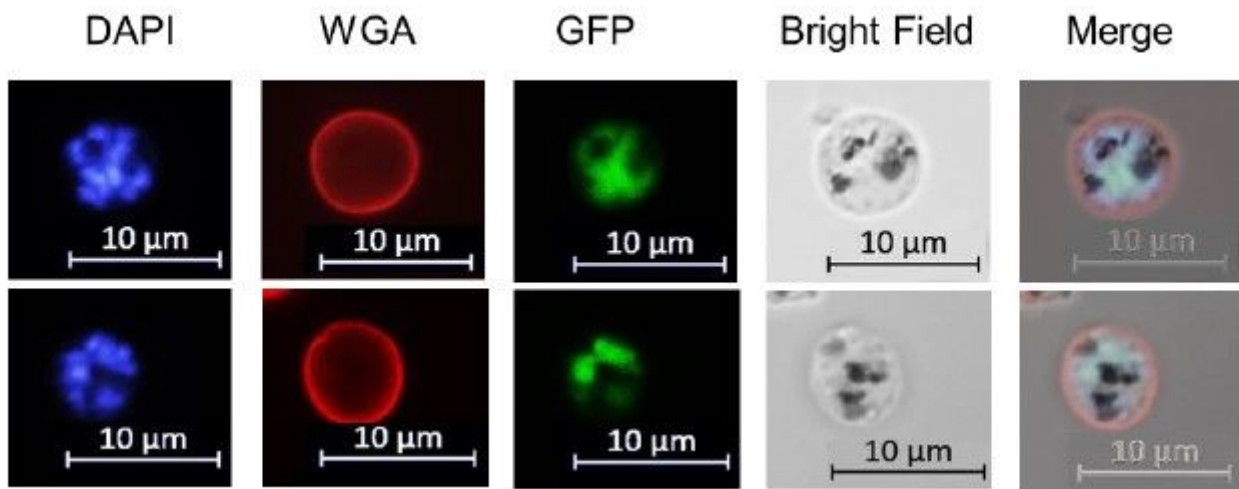


Figure 2

PfAP2-O-GFP-HA-DD24 is expressed in schizont stage parasites

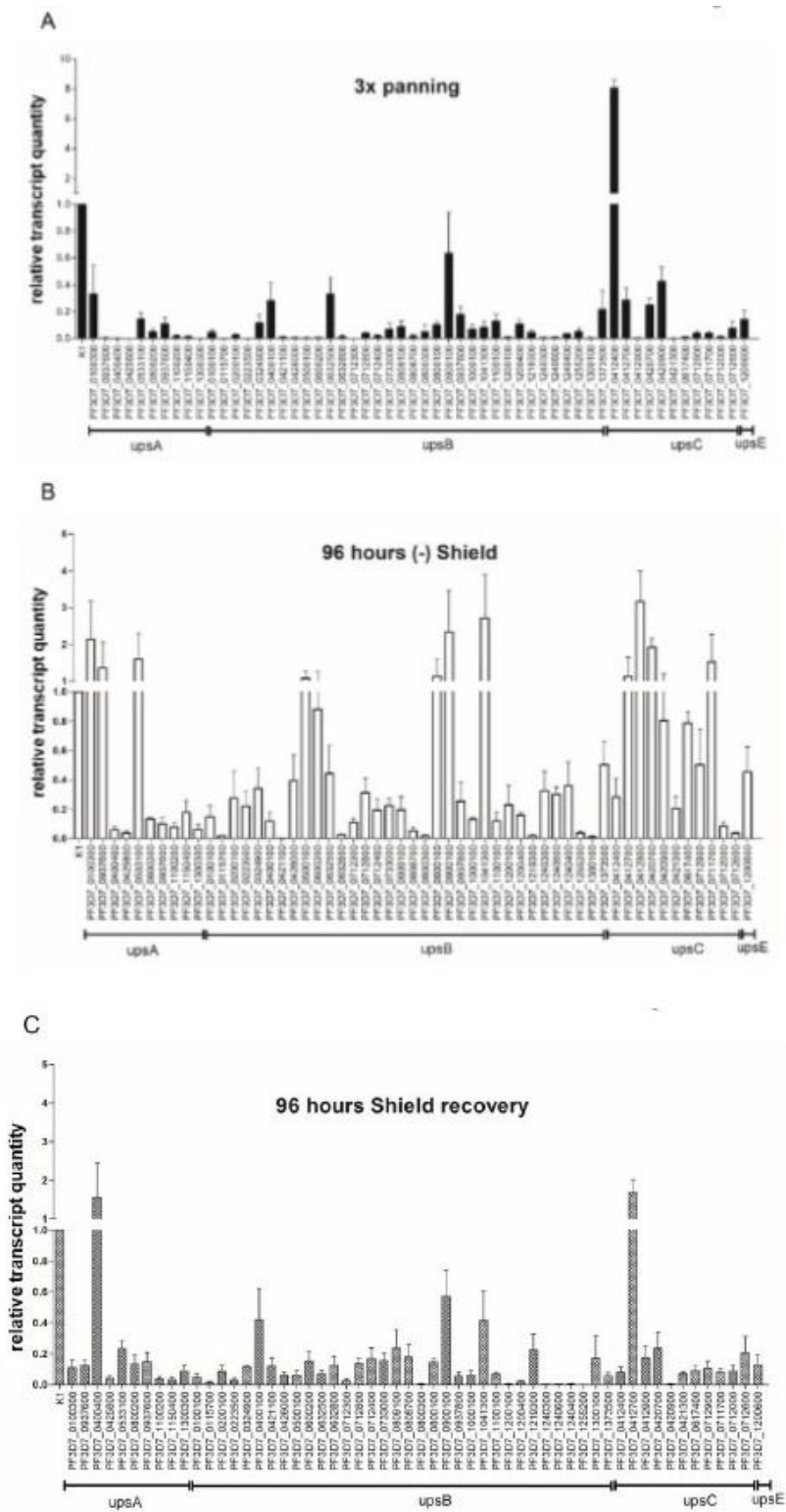


Figure 3

var gene transcription analysis during a transient knockdown in PfAP2-O-GFP-HA-DD24 parasites

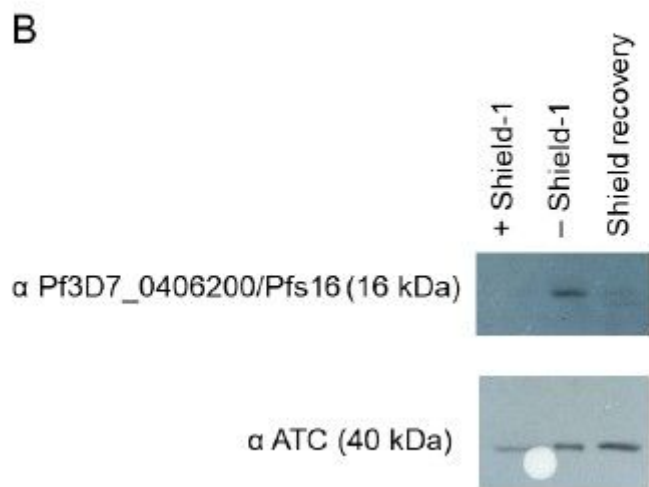
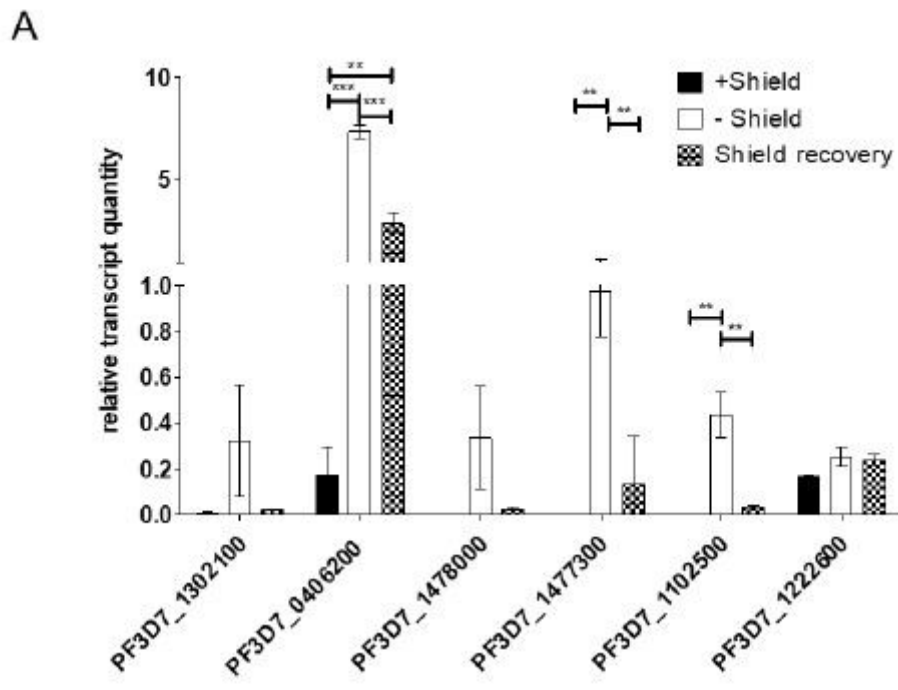
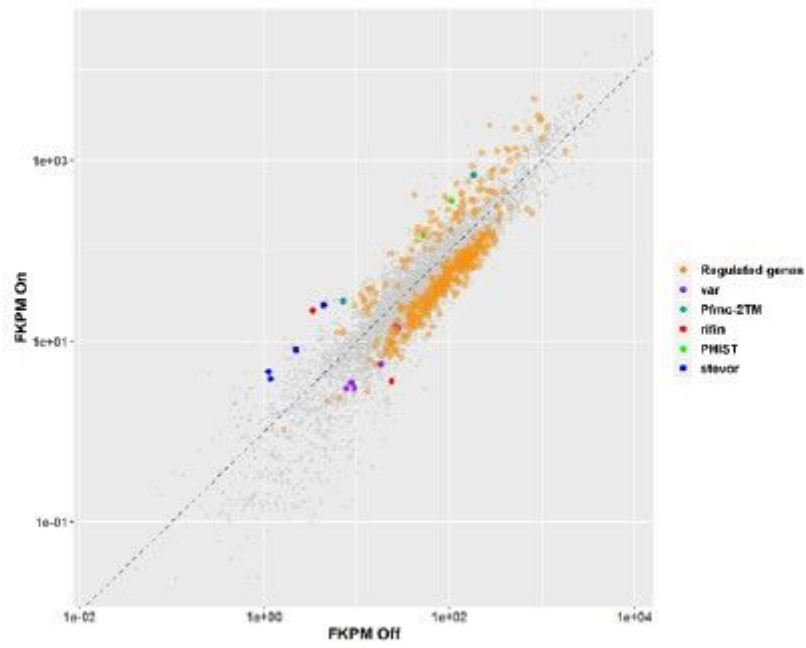


Figure 4

PfAP2-O-GFP-HA-DD24 is involved in the transcription/translation of gametocyte-related genes in *P. falciparum*

A

Figure 5



B

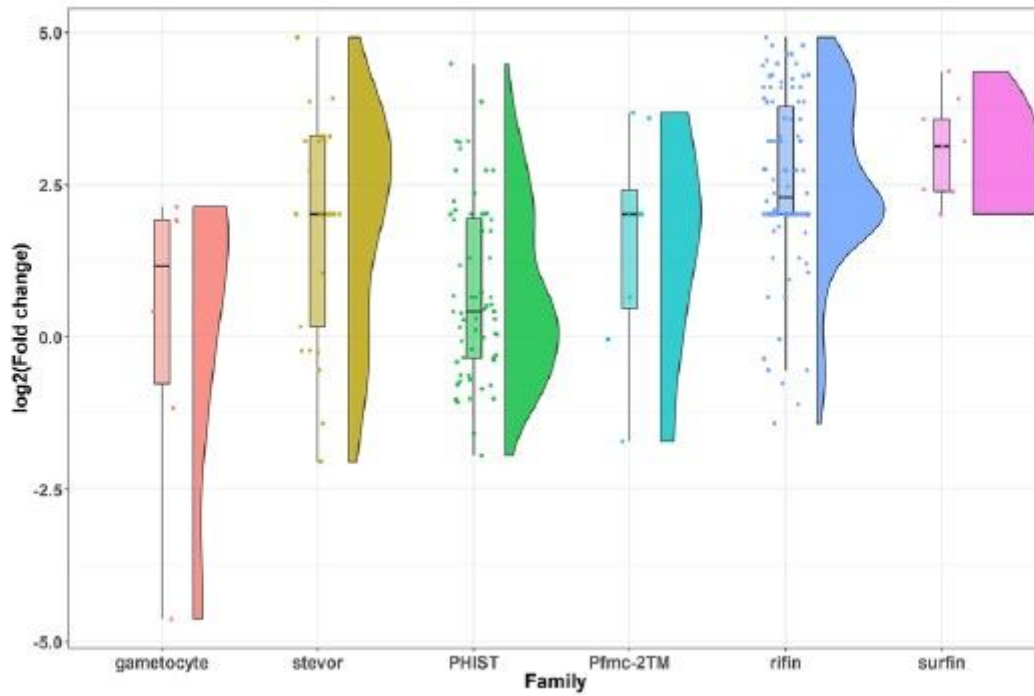


Figure 5

RNAseq analysis in PfAP2-O-GFP-HA-DD24 expressing or knocked down parasites in independent biological triplicates shows influence of PfAP2-O on variant gene transcripts

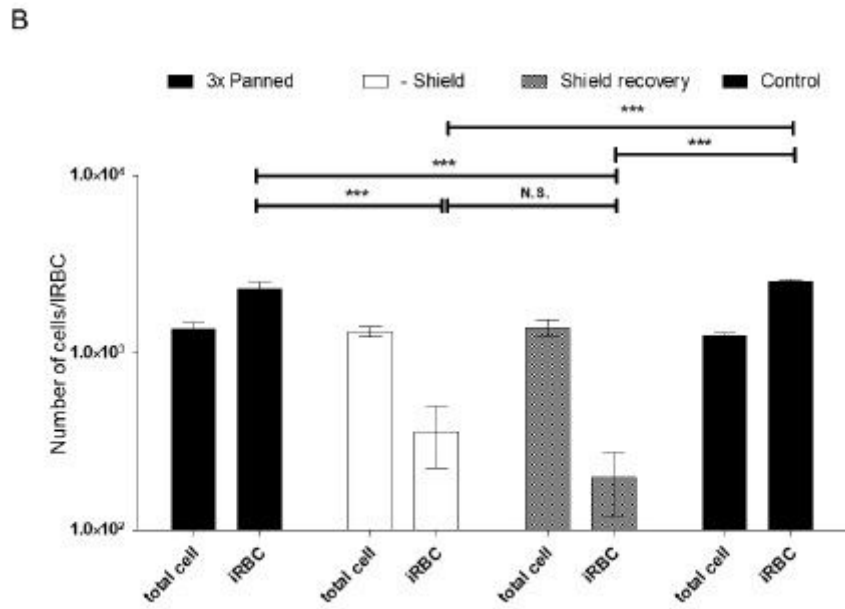
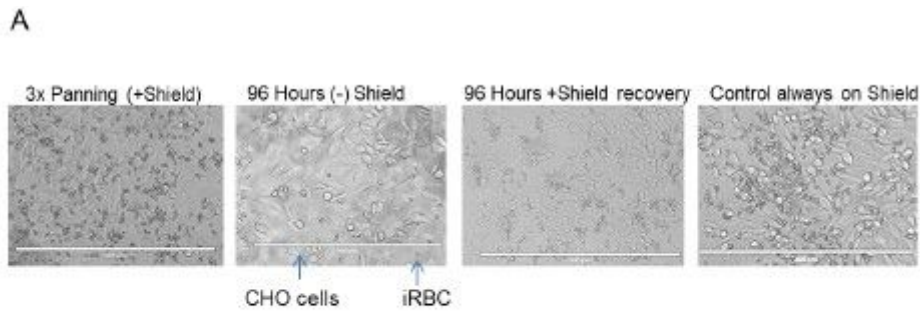


Figure 6

Adherent phenotype analysis shows decreased cytoadherence of IRBC during and after knockdown

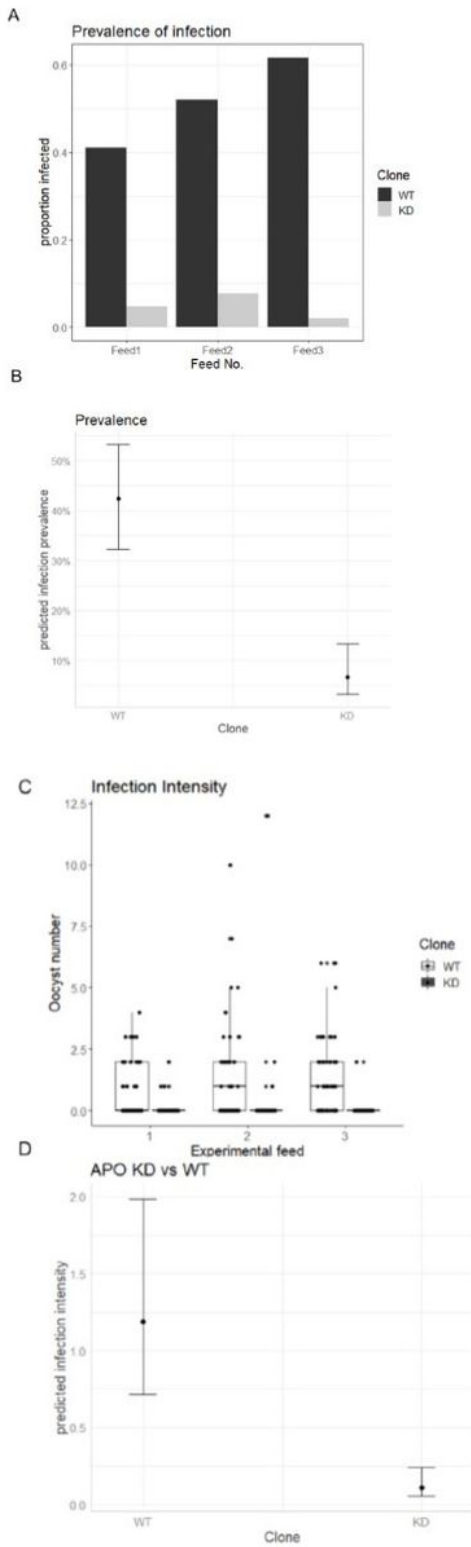


Figure 7

PfAP2-O is essential for *P. falciparum* transmission to *Anopheles coluzzii*

Supplementary Files

This is a list of supplementary files associated with this preprint. Click to download.

- [SupplementaryTable1.xlsx](#)
- [SupplementaryTable2.xlsx](#)
- [SupplementaryTable3RegulatedgeneswithTFmotifs.pdf](#)
- [SupplementaryTable4ProteomicAnalysis.pdf](#)
- [SupplementaryTable5RTPCRPrimers.xlsx](#)
- [SupplDataFile1.docx](#)
- [FigureS1.jpg](#)
- [FigureS2.jpg](#)
- [FigureS3.jpg](#)
- [FigureS4.jpg](#)
- [FigureS4a.jpg](#)
- [FigureS5.jpg](#)